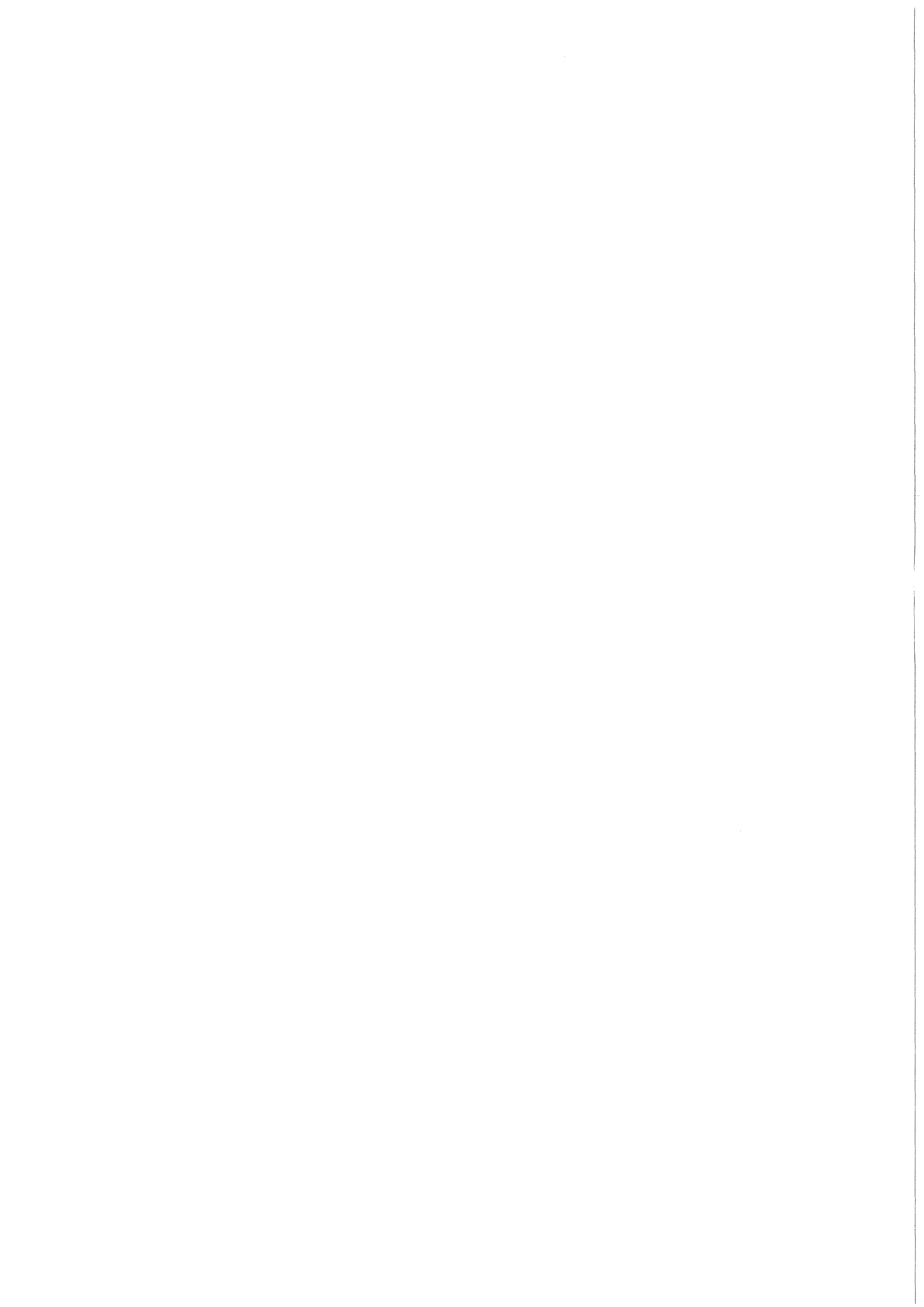


**KfK 3601**  
**November 1983**

# **Post-Accident Heat Removal Research: A State of the Art Review**

**U. Müller, T. Schulenberg**  
**Institut für Reaktorbauelemente**  
**Projekt Schneller Brüter**

**Kernforschungszentrum Karlsruhe**



KERNFORSCHUNGSZENTRUM KARLSRUHE  
Institut für Reaktorbauelemente  
Projekt Schneller Brüter

KfK 3601

POST - ACCIDENT HEAT REMOVAL RESEARCH:  
A STATE OF THE ART REVIEW

U. Müller, T. Schulenberg

Kernforschungszentrum Karlsruhe GmbH, Karlsruhe

Als Manuskript vervielfältigt  
Für diesen Bericht behalten wir uns alle Rechte vor

Kernforschungszentrum Karlsruhe GmbH  
ISSN 0303-4003

## Abstract

For a realistic assessment of the consequence of extremely unlikely reactor accidents resulting in core degradation or core meltdown key questions are how to remove the decay heat from the reactor system and how to retain the radioactive core debris within the containment. Usually, this complex of questions is referred to as Post-Accident Heat Removal (PAHR). In this article the research work on PAHR performed by various institutions during the last decade has been reviewed.

The main results have been summarized under the chapter headings "Accident Scenarios," - "Core Debris Accommodation Concepts," and "PAHR Topics." Particular emphasis has been placed on the presentation of the following problems: characteristics and coolability of solid core debris in the reactor vessel, heat removal from molten pools of core material, and core-melt interaction with structural materials.

Some unresolved or insufficiently answered questions relating to special "PAHR Topics" have been mentioned or discussed at the end of the particular Chapter. Problem areas of major uncertainty have been identified and listed at the end of the review article. They include the following subjects: formation of debris beds and bed characteristics, post dryout behaviour of particle beds, long-term availability and proper location of heat sinks, creep rupture of structures under high thermal loads.

## Eine Übersicht zu Forschungsergebnissen auf dem Gebiet der Nachwärmeabfuhr nach schweren, hypothetischen Unfällen

### Zusammenfassung:

Bei einer realistischen Abschätzung der Folgen schwerer aber sehr unwahrscheinlicher Reaktorunfälle mit Kernzerstörung oder Kernniederschmelzen bilden die beiden folgenden Themenkreise Schlüsselprobleme: a) Abfuhr der Nachzerfallswärme aus dem Reaktorsystem; b) sichere Verwahrung des radioaktiven Kernschutts innerhalb des Reaktorcontainments. Üblicherweise werden beide Themen unter der Überschrift "Nachzerfallswärmeabfuhr nach Unfällen (Post-Accident Heat Removal, PAHR)" zusammengefaßt. Im vorliegenden Artikel wird versucht, die Forschungsergebnisse der vergangenen zehn Jahre zu diesem Themenkreis in einer Übersicht darzustellen.

Die wesentlichen Resultate sind in den Kapiteln mit den Überschriften "Unfallabläufe", "Konzepte zur Rückhaltung von Kernschutt" und "PAHR"-Themen eingeordnet. Besonders ausführlich werden die PAHR-Probleme, Struktur und Kühlbarkeit von Partikelbetten, Wärmeabfuhr aus einer Kernschmelze und Wechselwirkung der Kernschmelze mit den Reaktorstrukturen abgehandelt.

Ungelöste oder unzureichend gelöste Einzelfragen zu den jeweiligen Themen sind am Schluß der jeweiligen Unterkapitel erwähnt oder diskutiert. Problemkreise, die mit größeren Unsicherheiten behaftet sind, wurden identifiziert und sind am Schluß der Übersicht aufgeführt. Es handelt sich hier im wesentlichen um die Fragen: Entstehung, Konfiguration und Struktur von Kernschuttablagerungen; Wärmeübertragung nach dem Austrocknen des Kernschutts; Langzeitverfügbarkeit der Wärmesenken; Kriechversagen von Reaktorstrukturen unter großen thermischen Belastungen.

Contents:	page:
1. Introduction	1
2. Accident Scenarios	4
3. Core Debris Accommodation Concepts	9
4. PAHR Topics	19
4.1 General Remarks	19
4.2 Debris Bed Formation	21
4.21 Debris Particle Size and Shape	21
4.22 Debris Settling and Dispersion	24
4.3 Secondary Criticalities	29
4.4 Distribution of Heat Sources and Fission Products	29
4.5 Heat Transfer from Debris Beds	34
4.51 Conduction Regime	34
4.52 Single-Phase Free Convection	37
4.53 Boiling Regime	43
4.54 Post Dryout Heat Transfer	55
4.6 Heat Transfer from Molten Layers	57
4.61 Single Phase Convection	57
4.62 Heat Transfer from Boiling and Bubbling Pools	61
4.7 Molten Pool Penetration into Substrates	65
4.8 Response of special Barrier Materials to Hot Debris	73
4.9 Mechanical Integrity of Structures under High Thermal Loads	81
4.10 Heat Transport from Hot Structures to Heat Sinks	82
5. Summary and Conclusions	85
Appendix	87
Figure Captions	88
List of Tables	89

## 1. Introduction

The safety of nuclear power plants is assured today by an overlapping set of rigid guide-lines, regulations and other measures. The primary goal of reactor safety strategies is accident prevention by reliable design and construction as well as reliable operation and maintenance of the plant. The potential threat by the radioactive inventory of the plant demands moreover a control of accidents including the limitation of the damage and limitation of release of radioactivity.

In order to prevent damage propagation with the ultimate consequence of uncontrolled release of radioactive material from a failing reactor containment to the environment, a balanced removal of the decay heat in the long time span following reactor accidents is a standard requirement for nuclear power plants.

For the class of design based accidents, heat removal is warranted by the emergency core cooling system implemented in the reactor design. The requirements for this system are regulated by licensing rules.

In this article mainly post-accident heat removal (PAHR) for the conditions of severe accidents with very low probability of occurrence will be discussed.

Generally these accidents are characterized by severely damaged cores or even the melt down of major parts of it (core melt down accidents). They are usually classified as hypothetical accidents, since for their occurrence all essential safety installations of the power plants shut down systems or heat sinks are postulated to fail.

In spite of the extremely low probability of their occurrence these accidents play a major role in the general discussions concerning the acceptance of nuclear power by the public, the reason being that in case of such an event considerable damage could arise. This may add a non negligible contribution to the overall risk of nuclear power plants. As a consequence for the risk assessment hypothetical accidents of all types of nuclear reactors are being analysed in detail, whereby particular attention is given to the core melt down accident and the related heat removal problem.

The article was written in order to identify unresolved or insufficiently treated problems in an advanced field of reactor safety research. In spite of the great number of different PAHR topics it has been tried to summarize the main results of each topic in individual chapters. Although in this review special emphasis is given questions related to the Liquid Metal Cooled Fast Breeder Reactor (LMFBR) particular subjects concerning the Light Water Reactor (LWR) are also outlined. Unresolved singular questions of a topic are addressed at the end of the particular chapter, problem fields of major uncertainty are listed in the summary of the article.

The article is organized in four main sections:

Section 2: Accident Scenarios

Section 3: Core Debris Accommodation Concepts

Section 4: PAHR Topics

Section 5: Summary and Conclusions

## 2. Accident Scenarios

For the liquid metal fast breeder reactor (LMFBR) mainly the following initiating events may lead to a disruption of the core /14, 15, 16/.

- a strong reduction of the coolant flow rate combined with a simultaneous failure of all shut down systems (ULOF - unprotected loss of flow accident),
- faults or malfunctions leading to an interruption of heat removal capability (even) after shut down,
- an uncontrolled reactivity increase combined with simultaneous failure of all shut down systems (UTOP - unprotected transient over power accident).

A loss of flow, caused e.g. by an Unprotected Loss of Off-Site-Power or an Unprotected Spurious Pump Trip, generates boiling of the coolant followed by clad melting on the fuel pins. The reduction of the coolant density by evaporation as well as the relocation of the molten clad material creates a reactivity ramp which - in an extreme case - may result in a sudden considerable energy release in the core. The fission energy is dumped within milliseconds as thermal energy into the core materials and causes fuel, steel and coolant to be melted and evaporated<sup>1)</sup>. An expanding gas bubble filled with sodium, steel and fuel vapor drives major amounts of molten fuel and steel of the upper part of the core into the sodium pool above the core. During an intensive interaction with the ambient coolant fuel and steel, the high temperature gases and molten

---

1) The relevant properties of reactor core materials in the PAHR phase are listed in the table of the appendix.

core material solidify into widely spread fine particles. These particles eventually settle on the cold internal structures of the reactor tank. A shut down of the nuclear reaction is achieved inherently by the discharge of fuel from the core. The molten constituents in the lower core structures may either be encapsuled by surface solidification forming a stable molten pool to be cooled down by the ambient coolant and the cold core structures. Or, the molten materials may penetrate the core in downward direction under the effect of gravity and residual decay heat generation. In the latter case the molten pool discharges into the lower plenum filled with coolant. Violent interaction between melt and coolant disintegrates the melt into small particles dispersed in the coolant which will eventually settle on internal structures or trays particularly installed for the retention of core debris. In order to assure the integrity of the vessel and thus the confinement of fission products in the primary reactor system, it has to be demonstrated that the decay heat can be transported by the coolant from the core and the structures loaded with debris to the heat sinks in the system.

The unprotected transient over power accident is postulated to be initiated by an uncontrolled removal of control rods from the core. A related significant increase in reactivity would cause rapid fuel melting and evaporation within the fuel rods and ejection of pressurized molten fuel into the coolant channels of the subassemblies. The fuel is immediately swept out from the core by the coolant under forced flow and thereby the reactor is brought to subcritical condition. The solidified fuel particles settle on the internal structures of the primary circuit of the reactor from where the heat is to be removed by the coolant to the heat sinks.

The only cause for severe core damage or even core melt down in Light Water Reactors, in particular Pressurized Light Water Reactors (PWR), is a Loss of Coolant Accident (LOCA) coupled with a complete failure or a very much delayed start of the emergency core cooling system (ECCS) /17, 18/.

The course of such an accident may be roughly characterized by the history of depressurization of the primary system.

For LOCA's caused by large breaks in one of the main coolant pipes the system pressure levels off quickly to the containment pressure (Low Pressure Course).

With the failure of the low pressure pumps of the ECCS postulated, the water content of the core would evaporate and the core would heat up and degrade. Then melting and slumping of major parts of the core would occur and result in the formation of a molten pool within the core region. Due to poor cooling conditions, the melt would entrain the lower part of the core, penetrate the core support structures and discharge into the lower plenum of the reactor vessel. A steam explosion may occur if the melt drops into the residual water. As a result, the melt disintegrates and, due to the fuel-coolant interaction, fuel granulates forms and sediment on the bottom of the pressure vessel. Under certain conditions the water within the particle bed will evaporate, the bed will become dry and melt. The core melt will attack the wall of the pressure vessel until it fails. The melt will then plunge into the concrete cavern beneath the pressure vessel and start to disintegrate thermally the concrete

of the basement. By these processes the integrity of the containment is threatened on one side by a build up of pressure in the containment atmosphere due to gas production during concrete decomposition and on the other side by a potential penetration of the melt through of the concrete basement.

Core melt down in Light Water Reactors could also occur at full system pressure due to transients initiated e.g. by the loss of off-site power and the simultaneous failure of the emergency power supply system. In this case the pressure within the primary system would increase until the pressurizer relieve valves open (High Pressure Course). As a consequence, primary coolant is leaking at a constant rate through the release valve. Thus the coolant is slowly evaporated from the primary system. Within a few hours the core is uncovered and the heat up phase of the core starts. By thermal and chemical reaction, the fuel elements may partly disintegrate and collapse forming a rubble bed on top of still cool and therefore intact core structures. As a later state of the transient, melting of the core debris occurs and a melt pool forms in the core region which, at a later stage, depletes into the lower plenum of the pressure vessel. It is still speculated, what the failure mode of the reactor vessel is like under melt attack and high system pressure. Nevertheless, a discharge of the melt into the reactor cavern beneath the pressure vessel is to be expected after a short time (about 30 min.). Due to the depressurization of the primary system the accumulators of the ECCS are activated and their water content is immediately dumped onto the melt in the cavern. The implications of these events are not yet fully analyzed but differences compared to the course of a core melt down accident at low system pressure are evident.

The different modes of the heat transport and their cooperation in the system are the subject of current research work, whose status will be reviewed in this article. It should be mentioned here already that in the case of LMFBR's the very favourable thermal hydraulic properties of liquid sodium provide a high potential for an in-vessel cooling of the core debris.

### 3. Core Debris Accommodation Concepts

The minimization of the radiological risk to an acceptable level requires the long-term retention of core debris within the reactor containment. In order to assure this, specially engineered safeguards have been proposed and some have been installed in prototype Fast Breeder Reactors. Such safeguards consist essentially of one or several trays capable of catching the debris from the core during a core melt down accident. These trays are either placed in the lower plenum of the reactor vessel (in vessel core catcher) or beneath the reactor vessel (ex-vessel core catcher). In the latter case, the melt through of the reactor vessel is accepted before the ex-vessel core catcher becomes activated. For the heat removal from the debris surface and from beneath the core catchers, active cooling by forced convection and/or passive cooling by natural convection is assigned.

Today, for reasons of simplicity and costs in-vessel core catchers are designed and build with steel. Formerly high melting alloys and metals have also been considered or used (e.g. Zirconium, Niobium, Tungsten etc.). In ex-vessel core catcher concepts actively cooled plates covered with high melting and resistant liner material (e.g.  $UO_2$ ,  $ThO_2$ , etc.) are employed to prevent melt penetration into the basement. Also, deposition of refractory sacrificial material (e.g.  $MgO$ ,  $Al_2O_3$  or Borax bricks) into the cavern beneath the reactor vessel is being considered. The latter concept is to be passive and based on an intended fast temperature reduction of the debris by penetration and dilution of the core melt into the sacrificial material. The heat from the diluted molten pool is then removed across its surface by convection, radiation and conduction to appropriate heat sinks within the containment.

The various design concepts have been discussed in more detail in references /6, 19, 20, 21, 22/. Some designs for core catchers in LMFBR's currently under construction or in the design phase are outlined next.

An ex-vessel core catcher pan has been placed in the reactor cavern of the German Loop Type Fast Breeder Reactor SNR-300. Its characteristic features are: A steel pan is covered with the resistant liner material depleted Uranium (thickness 8 cm). The pan is cooled from below by forced flow of liquid NaK through a system of cooling coils. The catcher pan is designed to intercept core melt accidents involving the whole core. The design character is very conservative and is based on the idea that the heat is removed from a molten debris layer covered by solid debris crusts to the overlying sodium pool and the underlying liner mainly by convection and conduction. A schematic arrangement is given in figure 1. A detailed description of the design is given by Friedrich /23, 24/ who also critically reevaluates the utilization of external core catchers for future LMFBR designs /25/.

An in-vessel core catcher is installed in the pool type LMFBR Super Phenix in France. A circular steel plate reinforced from below by a set of radial steel sheets is placed in the lower plenum of the reactor beneath the core support structure. The plate is completely surrounded by sodium. It is arranged to collect the fuel particles which, after a core melt coolant interaction, settle down in the sodium pool of the lower plenum. This conception takes into account the excellent heat removal capacity of natural convection in large

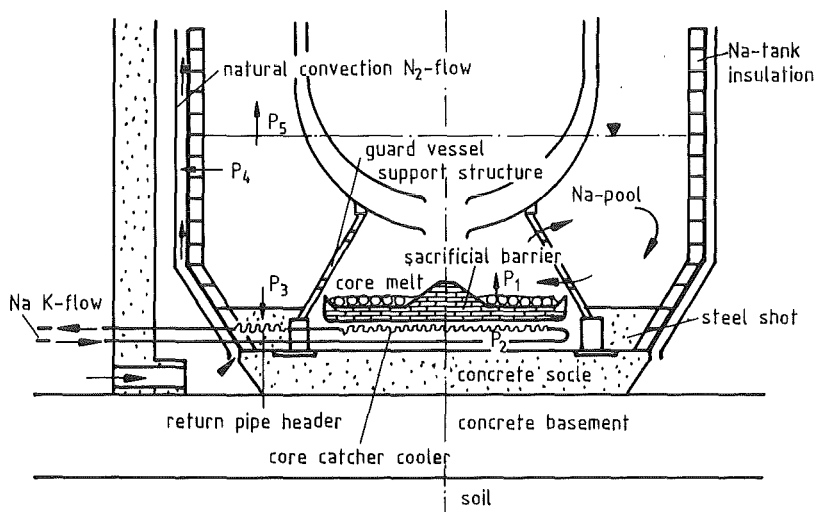


Fig. 1 SNR-300 core-catcher.

sodium pools. Moreover it is based on a shallow layer of debris particles on the plate from which the heat is removed by boiling heat transfer from within the debris bed to the surrounding sodium pool. The system is conservatively designed to sustain the load of the fuel of seven subassemblies of the reactor, but may well have a much larger capacity as best estimate calculations have shown. A schematic picture of the arrangement is given in figure 2. The characteristics of the design have been outlined by C. Le Rigoleur et al. in /26/.

A very similar in-vessel core catcher is assigned for the Demonstration Plant Fast Breeder Reactor CDFR in Britain. The specification for this core debris retention device is completely passive, based on natural convection within the sodium surrounding the structures of the core catcher. It consists essentially of a set of vertical stand pipes welded into conical tube plates with the top of each stand pipe bent over to prevent it from being blocked by falling molten fuel. The device resembles a bed of hollow nails whose cooling effectiveness is enhanced by the natural convection up through the standpipes. An illustration of the device is given in figure 3. This sophisticated, but in its conception very conservative, design can handle asymmetric loading of fuel debris piles up to 0.5 m high and the heat removal from a saturated debris bed is warranted by single-phase convection and conduction. The philosophy for this debris retention device has been discussed by Broadley et al. /27/.

Besides the efforts to provide appropriate engineered safe guards for debris accomodation, more recently the inherent retention

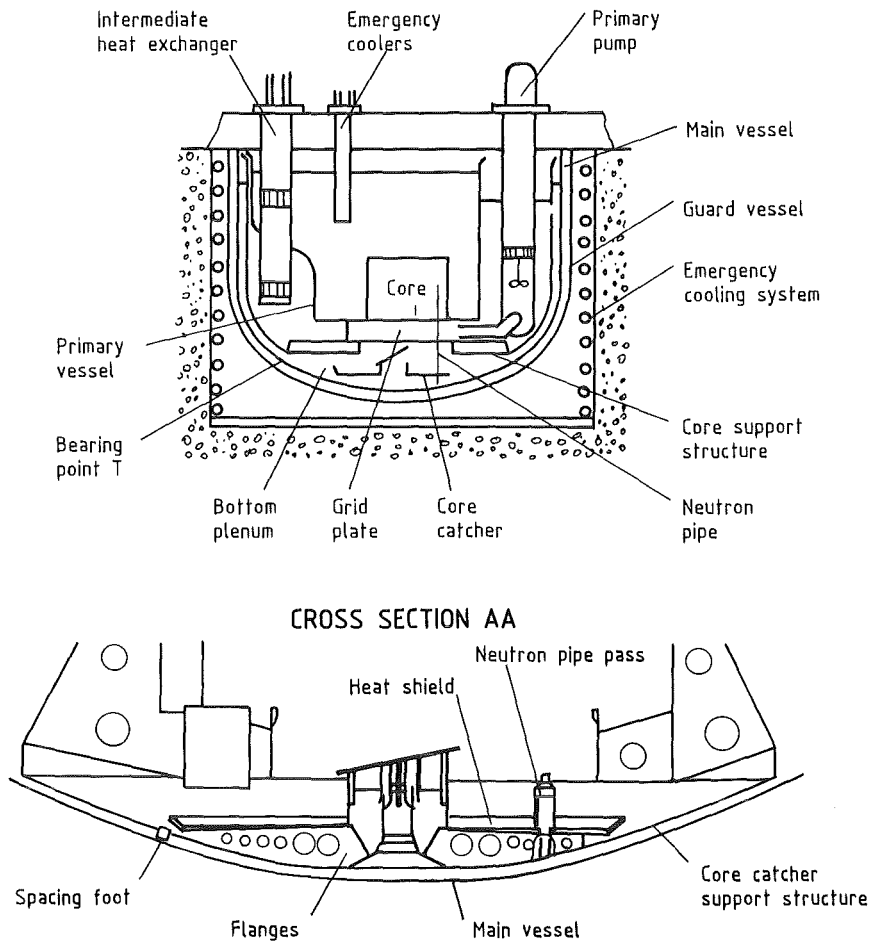


Fig. 2 The internal core-catcher in Super Phenix.

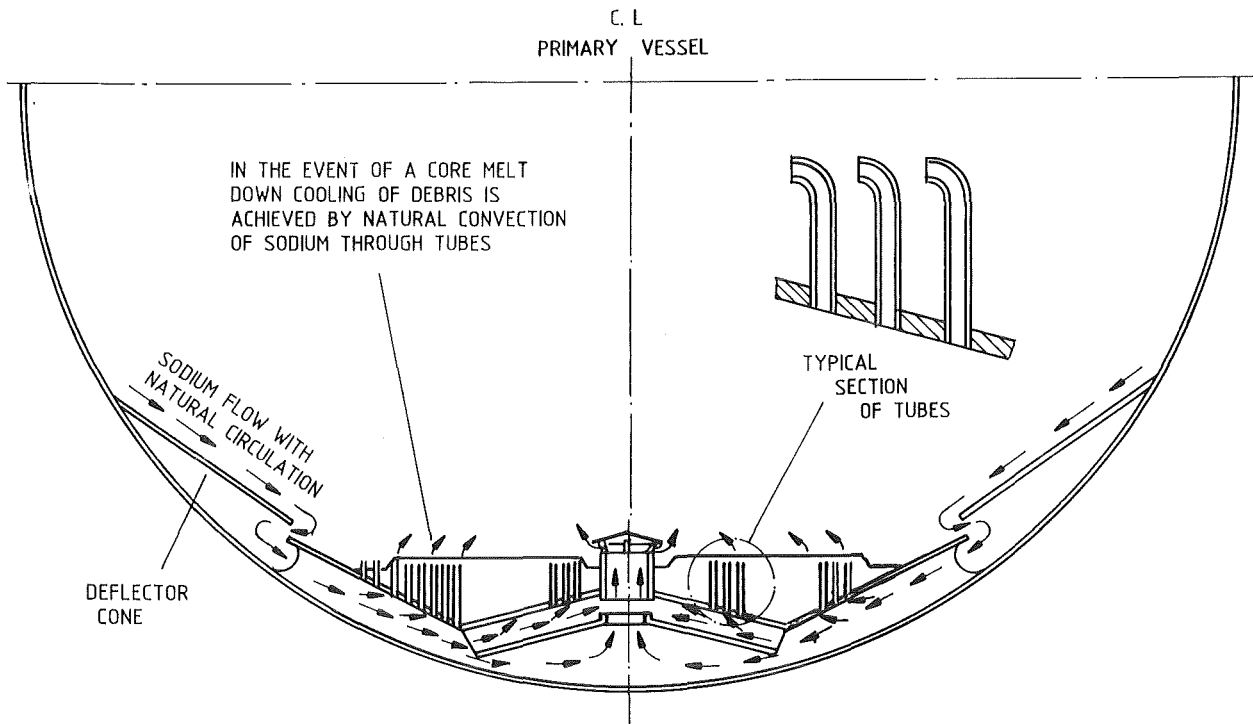


Fig. 3 In-vessel core-catcher in CDFR.

capability of the internal structures of LMFBR's have been investigated taking into account the favorable heat transport capacity of sodium. In a particular study concerning the coolability of core debris dispersed in the reactor vessel of the SNR-300 following a whole core Bethe Tait type accident, Vossebrecker et al. came to the conclusions that the heat can be transported from the debris layers to the emergency coolers by natural convection in the long term, and moreover that to a very high degree of probability the core debris can be retained permanently in the reactor vessel /28, 29/. The principal features of the in vessel natural circulation flow are displayed in figure 4. Vossebrecker and Friedrich /25/ have pointed out, however, that, for a completely deterministic proof of permanent debris accommodation, an early failure of the internal structures in the lower plenum resulting from pressure loads due to fuel coolant interaction or from an impact of a fuel jet onto the structure must be excluded. This problem needs further clarification. Regarding the retention capability of internal structures Glückler et al. have drawn similar conclusions from their analysis of core melt down accidents in large LMFBR's /30/.

As far as Light Water Reactors are concerned, investigations have been concentrated on exploring the retention capability of the reactor concrete foundation and in general, the containment for a core melt, see e.g. /31, 32/. Although presently a permanent containment of the core debris can neither be assured nor precluded, it has been proposed by best estimate calculations that the radiological damage is highly mitigated. These calculations take into account the relative benign behavior of core melt concrete interaction /33/ and predict that a containment failure by overpressuri-

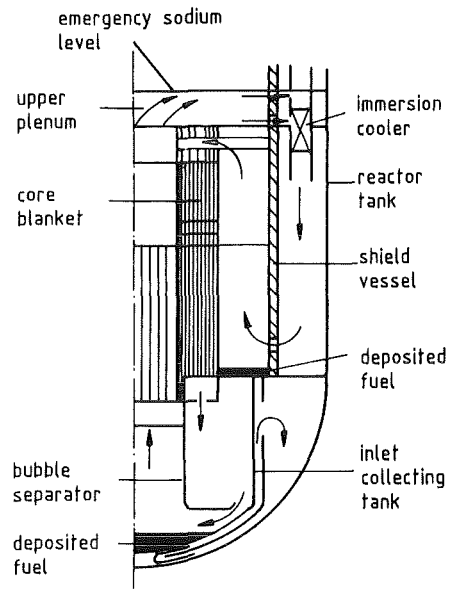


Fig. 4 In-vessel natural circulation flow in SNR-300 under PAHR conditions.

zation for the 1300 MW Class of PWR's must not be expected earlier than 3 to 4 days after a core melt down accident /31/. After this time the containment atmosphere is depleted from radioactive fission products by decay and by plate out processes of aerosols on the containment surfaces. Thus the leakage of fission products is expected to be small at the time when the containment fails.

In connection with the reassessment of the risk of some previously built PWR power stations in the United States, which suffer from an early design of volumetrically small containments recently speculative proposals have been made for retrofitting sacrificial core retention devices into the caverns beneath the pressure vessel. The core retention system is a bed of thoria rubbles on the floor of the reactor cavity. The rubble bed must be sufficiently thick and permeable to allow water to flow beneath a core melt laying on top of the bed and cool the melt from below by evaporation /34/. The system is to be completely passive. A principal sketch of this retention device is given in figure 5. Therefore, for the long term heat removal from the containment, condensers within the containment are proposed which are connected to natural draft cooling towers. At the Sandia National Laboratories, tests of this rubble bed core retention concept have been carried out. The result is that molten core material can be retained in flooded beds consisting of several layers of thoria and alumina pebbles /35/.

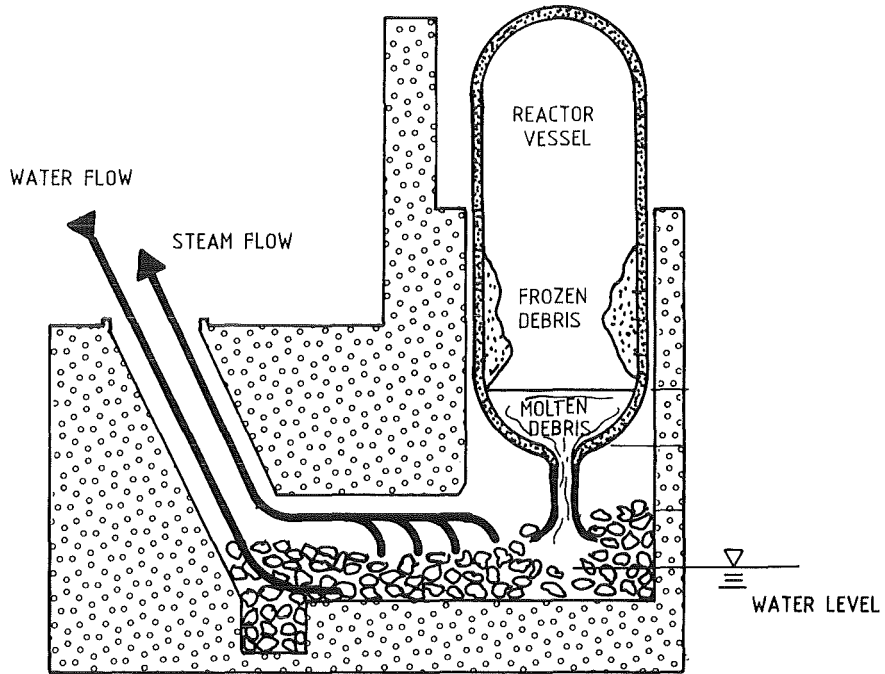


Fig. 5 Particle-bed core retention device.

## 4. PAHR Topics

### 4.1 General Remarks

In case of severe reactor accidents with core degradation or core meltdown the phase of decay heat removal is generally characterized by a sequence of transient and quasi-stationary thermal states of different temperature levels, which finally end in a stable steady state. PAHR research is mainly aimed at proving that this steady state of heat removal is achieved prior to a failure of the reactor containment. For this aim and furthermore for a most realistic risk assessment of core melt down accidents and for taking mitigating measures against expected damage a most precise knowledge of the heat transfer relations and their range of application is required. Determining conditions and bounds for the range of application mean that PAHR research is intended also for clearing the starting conditions as well as the transient states during the PAHR phase.

According to these aspects during the last decade, the following PAHR problems have been considered /1-5/.

1. Core debris generation and accumulation:
  - fuel-coolant interaction,
  - sedimentation of debris particles in the coolant,
  - physical properties of debris beds and core melts;
2. secondary criticalities;
3. distribution of fission products and heat sources;
4. heat transfer from heat generating particle beds:
  - single phase natural convection and two phase boiling heat transfer from saturated debris beds,

- dryout conditions,
  - post dryout heat transfer;
5. melting of debris beds by internal heat generation:
- sintering,
  - crust formation, crust stability,
  - melt front propagation;
6. heat transfer from heat generating molten pools:
- single phase natural convection,
  - pool boiling heat transfer;
7. interaction of core melt with structural materials:
- in-vessel structural material,
  - ex-vessel structural or sacrificial material;
8. thermal and mechanical loading of in-vessel structures and retention devices for core debris;
9. heat transfer from thermally loaded structures and retention devices to heat sinks,
10. pressure loading to the reactor containment by coolant vaporization and gas production due to thermal and chemical decomposition of structural materials.<sup>1)</sup>

The problems listed here have been identified for a long time /e.g. 37, 38/. New mechanisms that would additionally threaten safety barriers have not been proposed. Therefore it can be assumed that the catalog of key problems of the PAHR phase is complete.

---

1) This topic will not be discussed in this review article, but see e.g. Ref. /31, 36/.

However, in the past not all the problems have been treated to a depth according to their potential for risk reduction, as we shall see later. Limited knowledge and uncertainties in some areas are leading to over conservative assumptions in the general probabilistic risk assessment and are resulting in overly complex and expensive designs for debris retention devices (see Chapter 3).

With respect to safety, those problems should generally deserve the highest attention, which may result in an early failure of the internal debris retention devices, the reactor tank or the reactor containment. The assurance of the integrity of the safety barrier is not necessarily the only objective. Rather, for any realistic risk assessment, an accurate prediction of the elapsing time before failure may be as important since other mitigating effects or measures can be taken into account. Therefore, for predictive PAHR analysis, best estimate methods as well as moderately conservative methods are called for, depending on whether risk assessment or conceptual design work has to be performed.

## 4.2 Debris Bed Formation

### 4.2.1 Debris Particle Size and Shape

For a variety of accident events, the properties of the core debris will be determined by molten fuel coolant interaction processes (MFCI). Main features of these interaction processes are that either molten fuel is dropped or injected into the coolant (in-vessel interaction processes), or amounts of coolant stream or impact onto molten pools of core material (ex-vessel interaction processes). The two categories of situations have been simulated by several in-

pile tests and many out-of-pile laboratory experiments of different quantities of interacting materials in the range of grammes and several kilogrammes of molten material and up to several tens of kilogrammes of coolant /39-45/.

In these experiments mainly two mechanisms have been observed which govern the disintegration of coherent melts and the formation of small solid particles:

- hydrodynamic fragmentation by inertial, pressure and shear forces between the molten material and the liquid or vaporized coolant /46, 47/;
- thermal stress induced fragmentation of solidified submersed melt surfaces and melt globules /39, 48, 49/.

Based on the great number of experiments a sound knowledge on the particle size distribution of core debris generated by MFCI's exists. From figure 6, one can see that 70 to 80 % of the total mass involved in a MFCI is disintegrated into particles of diameters less than about 0.8 mm. The distribution of the particle sizes can be described approximately by a log-normal law, the mean diameter varying between say 0.1 and 0.8 mm /39/.

In general the following observation has been made: the more intense the heat transfer was between the melt and the coolant, and thus the higher the conversion rate of thermal and mechanical energy, the larger was the amount of very small particles /42, 50/. As far as the particle shape is concerned, post-test optical examinations indicate that, in relatively mild interactions, a large number of jagged oxidic

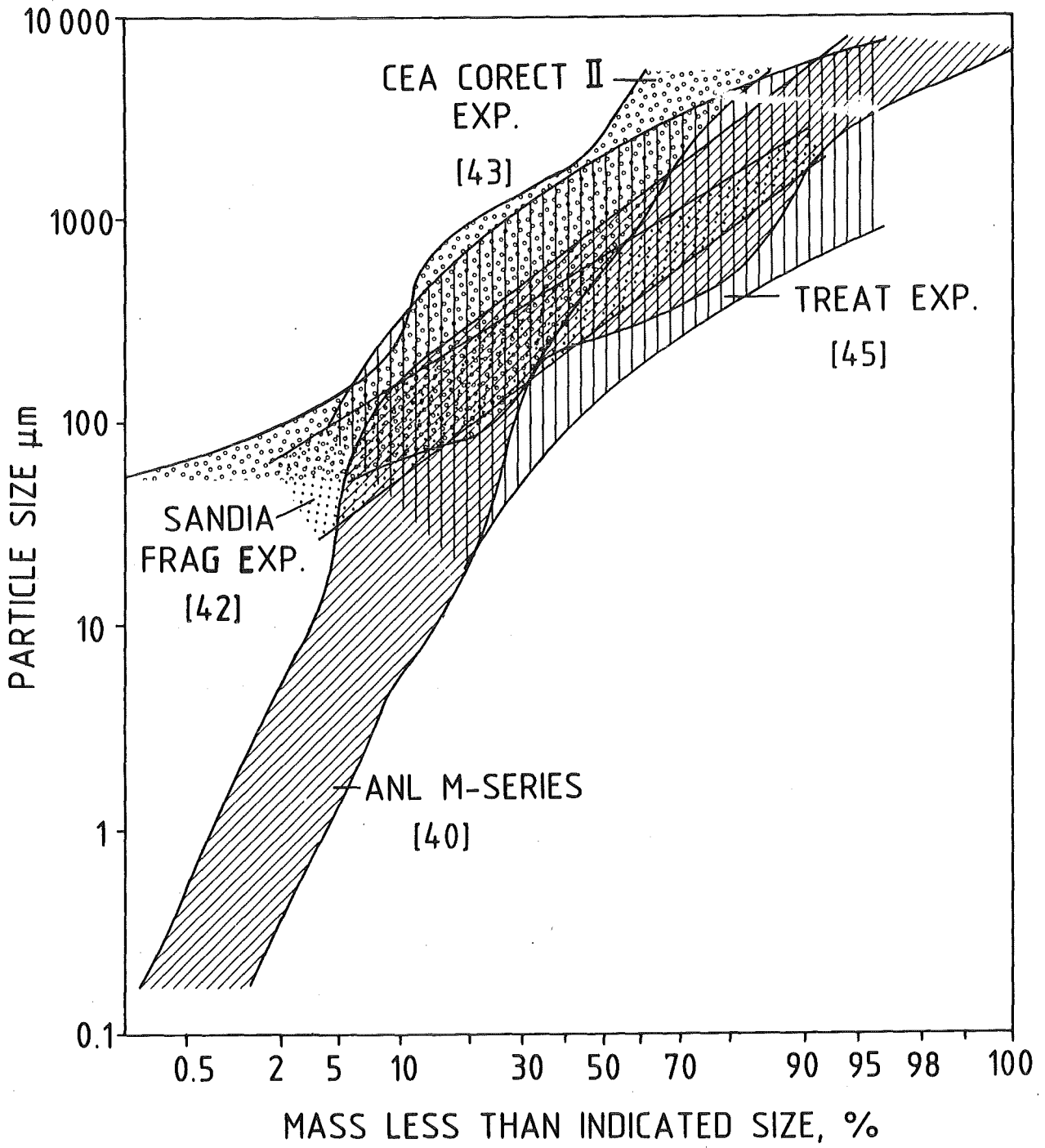


Fig. 6 Particle size distribution obtained from fuel coolant interaction experiments.

particles are generated due to stress induced fragmentation, while fragments with a smooth surface and with spherical cavities and inclusions are found predominantly after intense MFCI's /39, 40/, where hydrodynamic fragmentation prevails.

The particle size distribution and particle shape determine essentially the porosity and thereby the thermal-hydraulic properties of the particle beds, namely the permeability and the effective heat conductivity of a saturated particle layer.

Debris piles in the core region of LWR's can be generated by a thermal and chemical degradation as well as by partial melting of fuel pins followed by a collapse of the rod assemblies. All these events actually happened during the Three Mile Island accident. Although it is believed that the main phenomena of such processes are recognized little is known about the quantitative relations. A first view of the type of LWR debris resulting from severe in-pile transients has recently been given by Hobbins et al. /51/. The authors summarize that particle size distribution of debris are found to vary strongly with the severity of the rod damage produced. In general, greater rod damage produces smaller particle sizes.

For further characterization of rubble beds due to core degradation and collapse, in-pile and out-of-pile experimental research is needed. Corresponding research programmes have been launched /52,53/.

#### 4.22 Debris Settling and Dispersion

The coolability of debris piles depends on its geometrical shape and its internal structure. Both influencing factors are determined

by the settling of the small fuel and steel particles through the coolant under the effect of gravity and turbulent swirling of the coolant. Primarily three aspects have been investigated in some detail:

- The formation of conical debris piles by settling small particles from a local source through a pool of liquid onto a collector /54/.
- The formation of particle stratifications in the debris beds due to differences in the sedimentation velocities of particles of different sizes and due to induced secondary flows /54, 55/.
- Levelling of saturated debris piles by boiling of the coolant in debris beds /54, 56/.

For reactor-prototypical heights of fall and for local injection of a cold stream of particles of typical weight and size into a pool of water, Alvarez and Amblard have obtained the following experimental results /54/:

- Conical piles with angles of inclination up to 23 degrees are formed depending on the particle size.
- Small heights of fall and small particle sizes ( 0.2 mm) foster the formation of piles with steeper flanks.
- The bigger particles settle predominantly near the centre of the pile, while the fines are carried to the periphery by an induced secondary flow.

With respect to a coolability of the debris bed by boiling heat transfer, the relatively poor leveling due to the free fall of the particles would pose a serious problem, but one must be aware of the fact that local injection of a cool particle quantity into a

pool is rather unprototypical compared to the accident situation. Under such conditions, violent interaction between molten fuel, and the coolant would generate a vigorously stirred pool. The settling and leveling process will then lead to more uniform dispersions of the debris. However, MFCI-experiments in a typical scale, that would better simulate the initial conditions, are out of sight.

On the other side, in case of unfavourable shapes of the debris piles, self leveling of inclined bed surfaces has been observed due to boiling of the coolant inside the heat generating particle bed /55, 56/. This process has proved to be very effective. Depending on the power density even conical piles with large angle of inclination, up to 23 degrees, level out to nearly flat layers (angles of inclination of less than 2 degrees) after a time in the order of hours. Subcooling of the saturating coolant as well as stratification of the bed reduces the boiling effectiveness and therefore increases in general the times needed for complete leveling.

In some recent MFCI experiments Chu et al. /41, 42/, employing molten  $UO_2$  and sodium in the 20 kg scale, have demonstrated that the spatial particle size distribution is stratified vertically, i.e. the larger particles are located near the bottom while the finest are on top. The effect is displayed in figure 7, in which the bed void fraction is plotted versus the distance from the bottom.

Depending on the particle size distribution, the permeability of the bed may vary by as much as a factor of 20 from bottom to the top. As we shall see later, particle stratification has a major influence on the heat removal from the bed by single- or two-phase flow natural

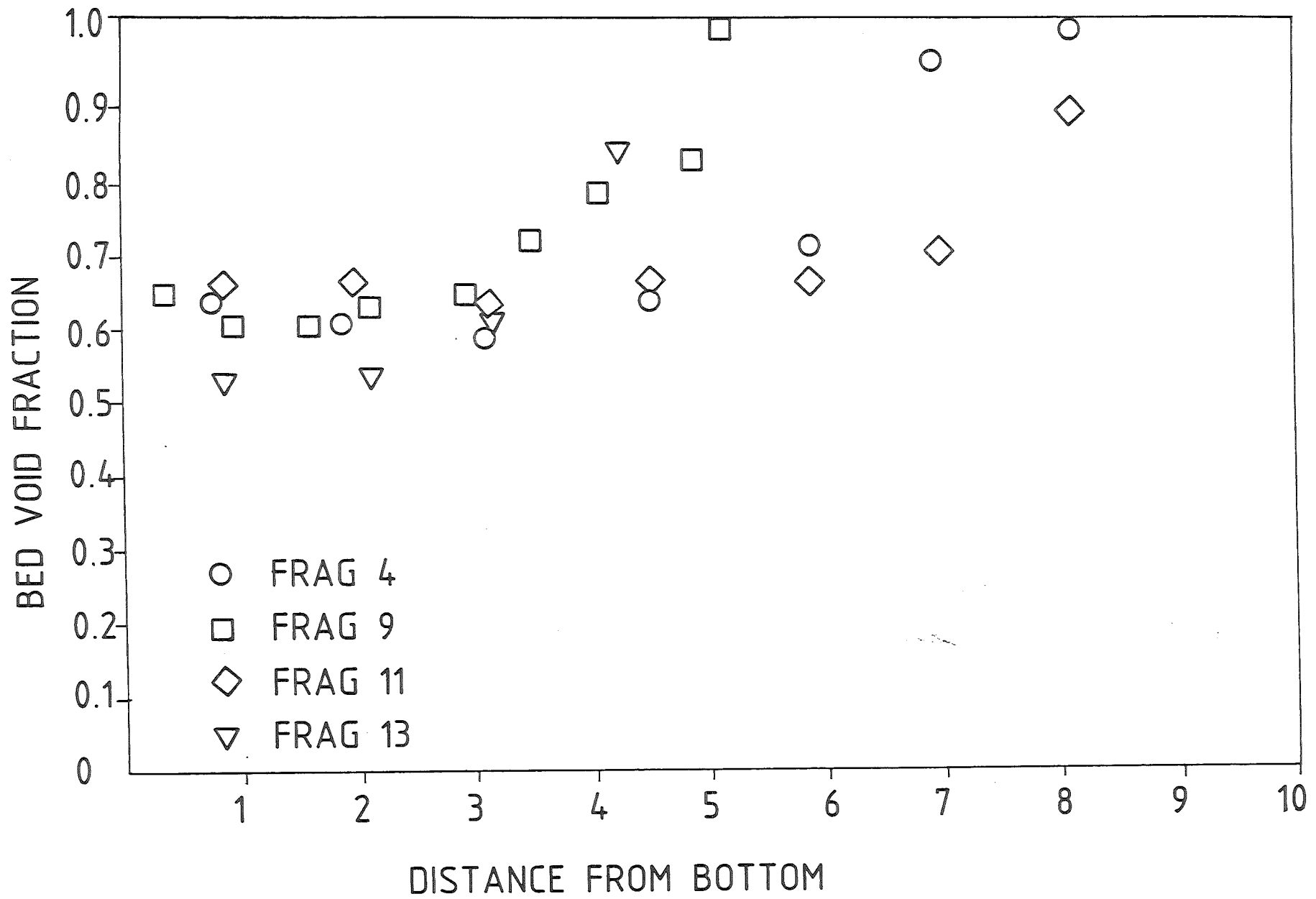


Fig. 7 Void fraction in a stratified particle bed /42/.

convection. Although the phenomenon of stratification in fuel particle beds is clearly demonstrated by these experiments and models for the prediction have been proposed /57/, it is an open question, what typical strength of stratification would occur under accident conditions, e.g. in the reactor tank.

Inadequate attention has been paid so far to the problem of debris carry over from the reactor vessel into the primary system piping and components of loop type reactors /58/. The question is directly related to the integrity of the piping system. In a theoretical investigation of this problem for the Fast Flux Test Facility (FFTF) and the Clinch River Breeder Reactor (CRBR), Tsai has stated that all the core debris swept out into the primary heat transport system piping will not remain in suspension and will form a particulate debris bed on the piping walls /59/. Regarding the quantity of the particle carry over he concludes that the heat can be removed from the debris settled on the piping walls.

The question, whether chemical reactions between  $UO_2$  and Na (Uranate formation) can change the debris bed structure in the long run has been raised in the past but has not been investigated.

In summary there are some uncertainties regarding the prototypical formation and structure debris beds. Additional research in this field is needed.

#### 4.3 Secondary Criticalities

Since the fuel in the core of a Fast Breeder Reactor is not arranged in a most reactive configuration, uncontrolled compaction of core material can enhance the reactivity beyond criticality. In the context of PAHR, it is widely accepted that, as a consequence of a core melt down accident, critical accumulations of core debris outside the core are generally extremely unlikely. This has been discussed by considering the reactivity of different geometries of debris piles /6, 19/. Nevertheless these facts have to be proved for different reactor designs individually, since the reactor cavern may shape the debris pile and influence the neutron economy. For the prototype reactors SNR 300 and the SUPER-PHENIX I, it has been shown that secondary criticalities outside the core region can be excluded for the PAHR-phase /28, 60, 61/. In both cases the proof is essentially based on the effect of fuel dispersion by fuel coolant interaction and on a final distribution of fuel masses in relatively thin debris layers of subcritical geometry.

#### 4.4 Distribution of Heat Sources and Fission Products

The contribution of the different fission products to the total decay heat generation as a function of time is well known. Various programs are available for prediction as for instance the codes CINDER (LA) /62/, RIBD (HEDL) /63/, ORIGEN (ORNL) /64/.

More important than the contribution of the different elements to the overall decay heat is the distribution of the fission products in form of chemical compounds or in elemental form within the

debris, the coolant, the cover gas or as a plate-out on internal surfaces of the primary system or the containment.

Best estimate evaluations have been made for the distribution of the fission products based on the thermal and chemical properties of the constituents of the involved materials /65, 66/. These estimates are supported and in part modified by experimental findings /67, 68/. For a specific case simulating a burnup of 100 000 MW d/t of fuel from an LMFBR, the following distribution of the elements was found experimentally by Parmentier and Damien /68/.

- The oxidic phase contains the rare earth elements Zirconium, Niobium and Yttrium completely which contribute 37 % of the total decay heat.
- The metallic phase dissolves the noble metals ruthenium, rhodium, palladium and molybdenum and contributes thereby 17 % of the residual power.
- The noble gases mix with the covergas and the halogens (Br, I), the chalcogenes (Se, Te), the pnictogens (As, Sb), the alkaline (Cs, Rb) elements as well as cadmium and silver are highly or in part soluble in sodium. They represent all together 46 % of the initial decay heat.

The data given above correspond to a residual power density of 1.72 W/g in the metallic phase and of 1.82 W/g in the oxidic phase.

Together with chemophysical consideration and the available codes, data from such integral experiments provide a reasonable base for assessing an envelope for the distribution of the heat sources. One

must keep in mind, however, that the actual distribution of some fission products such as Ag, Sn, Ru, Te, Ba, Sr and others may vary, depending on the history of the accident and the achievement of equilibrium states between different chemical compounds and solvents.

For LWR's, the redistribution of fission products is different because of the oxidizing steam atmosphere and the presence of the circaloy cladding on the fuel pins. The formation of eutectic compounds containing  $UO_2$  and Zr reduces the melting temperature of the mixed fuel-clad debris to less than 2500 K. For LWR conditions release rates of fission products have been measured by Albrecht and Wild /69/ by heating prototypical debris up to the melting point. Typical release rates in (%/min) for a reference temperature of  $T = 2673$  K are given in table 1 (others can be found for different temperatures in /69/). According to Albrecht and Wild the mass release during a time interval  $\Delta t$  at a particular constant temperature  $T$  can be calculated according to relation  $m = m_0 [1 - \exp(-\alpha \Delta t)]$ , where  $m_0$  is the element inventory at the beginning of  $\Delta t$  and  $\alpha$  is the specific release rate at a temperature  $T$ .

By employing a best estimate temperature history of the core debris and the empirical mass release relation, the sources of decay heat in the containment can be predicted. Reimann /70/ has calculated on the basis of the Origen Code the heat source distribution during a core melt down accident for a typical burnup of an LWR of the 1300 MWE class at the end of one period of operation, when fuel elements are to be changed. The history of decay heat source term and the temperature history of the core debris are displayed in

Release Rate <sup>a)</sup>		Release Rate <sup>a)</sup>	
Element	Steam	Element	Steam
Mo	0.01 <sup>b)</sup>	Fe	0.1
Ru	<0.001	Co	0.09
Ba	0.05	Cr	0.08
Zr	0.001	Mn	1.0
Ce	0.001	Sn	1.4
Nd	0.001 <sup>b)</sup>	U	0.02
Np	0.001 <sup>b)</sup>		

a) estimated uncertainty:  $\leq$  factor 2

b) extrapolated from 2300 °C

Table 1: Release rates of fission products from a core melt in (%/min) for T = 2400 °C after Albrecht and Wild /69/.

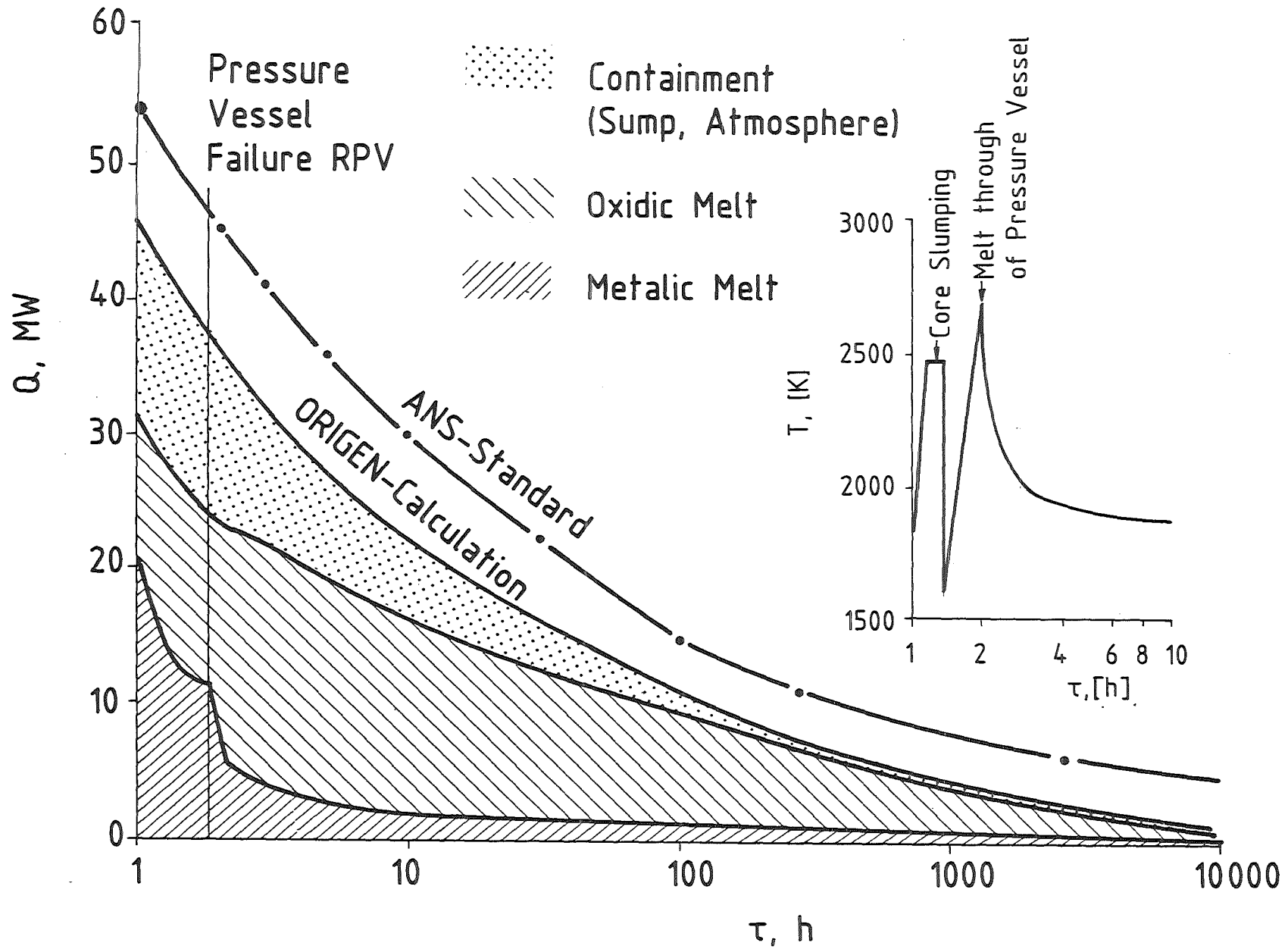


Fig. 8 Distribution of heat sources during a LWR-core-melt-down accident, after /70/.

figure 8. During the first few hours a strong shift of heat sources occurs from the metallic phase to the oxidic phase. This effect is due to the oxidation of the metals in contact with steam at high temperatures. Furthermore, the fission products released to the atmosphere contain 32 % of the decay heat sources at the beginning but after 100 hours only 17 % while the melt contains at this time 83 % of the decay heat sources. It is worth mentioning that the values of the ANS-standard curve for the heat source are in general clearly above the values of the best estimate calculations.

#### 4.5 Heat Transfer from Debris Beds

Heat Generating saturated particulate beds can be cooled by conduction, convection or by boiling of the saturating coolant inside the bed. The following two questions are of practical interest for the design or evaluation of debris retention devices.

- What are the heat fluxes across the boundaries of the debris bed i.e. in upward, downward and sideward directions?
- What are the limiting conditions for a steady heat removal by the different modes of heat transfer?

##### 4.51 Conduction Regime

The temperature and heat flux distribution in heat generating particulate beds caused by pure heat conduction can in principle be predicted, if the spatially averaged thermal properties of the saturated porous body is known. These properties depend on the particle size, the size distribution, the stratification of size distribution and the quality of particle and phase contact. In currently dis-

cussed models for the heat conductivity or heat diffusivity of porous bodies, these influencing quantities are only taken into account by means of a porosity parameter, and, in case of more sophisticated considerations, by means of anisotropy factors.

All these quantities can only roughly be assessed for debris beds generated under accident conditions. The inherent difficulty to precisely characterize the integral properties of debris beds has led to a dual procedure in deriving models for the heat conductivity. On the one hand, empirical and semi-empirical formulas have been derived and experimentally confirmed /71, 72/, and, on the other hand, more recently efforts are being made to provide rigorous upper and lower bounds, based on more general properties for the porous body, as for instance porosity and anisotropy parameters /73/. This latter approach deserves even more attention with respect to design oriented accident analysis.

In table 2, some relations for the heat conductivity in two component porous bodies are given. They are selected in the context of current PAHR research. A more general compilation and discussion of different models can be found in /74-76/. It shall be mentioned here that the relation after Kampf and Karsten was employed to evaluate the relevant Sandia in-pile tests on debris beds cooling /77, 78, 79/. The experimental data for the temperature distribution in the conduction regime were found in good agreement with the prediction by the Kampf-Karsten relation.

Kämpf-Karsten /71/:

$$k_b = k_d \left| 1 - \frac{\varepsilon (k_d - k_c)}{k_c + \varepsilon^{1/3} (k_d - k_c)} \right|$$

$k_b$  - heat conductivity in the average

$k_c$  - heat conductivity of continuous phase (liquid)

$k_d$  - heat conductivity of dispersive phase (solid)

$\varepsilon$  - porosity (volume fraction of continuous phase)

Schulz /72/:

$$\varepsilon = \frac{k_d - k_b}{k_d - k_c} \left( \frac{k_c}{k_b} \right)^{1/3}$$

Zehner-Schlünder /75/:

$$k_b = k_c \left\{ 1 - (1 - \varepsilon)^{1/2} + 2(1 - \varepsilon)^{1/2} \frac{1}{Y} \left[ \frac{Y-1+B}{Y^2} \ln \frac{k_d}{Bk_c} - \frac{B+1}{2} - \frac{B-1}{Y} \right] \right\}$$

with  $Y = 1 - \frac{k_c}{k_d} B$ ,  $B$  - particle shape factor

lower and upper bounds after Cook + Peckover /73/:

$$k_{M2} < k_b < k_{M1} ; \quad k_c > k_b$$

$$\frac{1}{k_{M1} + 2k_c} = \frac{\varepsilon}{3k_c} + \frac{1 - \varepsilon}{k_d + 2k_c}$$

$$\frac{1}{k_{M2} + 2k_d} = \frac{\varepsilon}{k_c + 2k_d} + \frac{1 - \varepsilon}{3k_d}$$

Table 2: Thermal conductivity relations for isotropic particle beds.

#### 4.52 Single-Phase Free Convection

Conditions for the transition from the state of pure heat conduction to single phase convection in saturated particle layers are fixed by three typical groups. These groups are the internal and external Rayleigh number, characterizing the heat source distribution and the temperature difference between the lower and upper side of the porous body, and furthermore two Biot-numbers, characterizing the thermal boundary conditions by relating the local heat flux and the local temperature at the boundaries.

The groups are defined in table 3.1. Regarding the onset of convection, the following qualitative trends can be stated: For largely homogeneous conditions, the onset is characterized by fixed values of the two Rayleigh numbers (critical Rayleigh numbers) /80/. In particular, increasing external Rayleigh numbers (i.e. increasing the temperature differences between the lower and upper boundary) lead to smaller critical internal Rayleigh numbers.

Limiting the heat flux at the boundaries by finite heat conductivities of the confining walls reduces the values of the critical internal Rayleigh numbers /81/. The same effect is found if parts of the surrounding walls are permeable for the liquid or if the porous layer is superimposed by a liquid layer /82/. Moreover, for any non-homogeneous distribution of heat sources, material properties or non-homogeneous boundary values will reduce the threshold for the onset of convection.

Group definitions:

$$Ra_I = \frac{g\beta_l K}{\kappa_m \nu_l} \cdot \frac{Qh_p^3}{2\lambda_m} \quad \text{internal Rayleigh number}$$

$$Ra_E = \frac{g\beta_l KH}{\kappa_m \nu_l} \cdot (T_0 - T_1) \quad \text{external Rayleigh number}$$

$$Ra_f = \frac{\beta_l g (T_M - T_1) h_l^3}{\lambda \kappa} \quad \text{external Rayleigh number of the overlying fluid layer}$$

$$Bio = \frac{\alpha h_p}{\lambda_m} \quad \text{Biot number}$$

$$Nu = \frac{Q \cdot h_p^2}{2\lambda_m (T_0 - T_1)} \quad \text{overall Nusselt number}$$

$$Nu_p = \frac{Q \cdot h_p^2}{2\lambda_m (T_0 - T_M)} \quad \text{Nusselt number of the porous layer}$$

$$Nu_f = \frac{Q h_p h_l}{\lambda (T_M - T_1)} \quad \text{Nusselt number of the fluid layer}$$

$$\eta = \frac{q}{q_{tot}} = \frac{q}{Qh_p} \quad \text{percentage downward heat flux}$$

Table 3.1 Group definitions of Table 3.2.

The heat transfer from internally heated particle beds has been investigated mostly for the special case of an adiabatic lower boundary. Results are available from laboratory experiments by means of Joule heating of the liquid phase /82-85/ or by inductive heating of the solid phase of the particle bed /86-88/. Heating by nuclear fission has been used in a set of in-pile experiments at the Sandia Laboratories, in which enriched  $UO_2$  pebbles and sodium as the liquid were employed /77-79, 89/.

The heat transfer from particle beds can essentially be described by two dimensionless groups, the Nusselt number and the internal Rayleigh number (see table 3.1 for definitions). It can be seen from table 3.2 and figure 9 that major differences exist between the correlations as given by the different authors. In particular, discrepancies exist between the heat transfer correlation obtained from in-pile tests with prototypical reactor materials /78, 89/ and from out-of-pile tests with simulant materials. Although the potential of heat removal from particle beds by single phase convection is of minor relevance for PAHR situations compared to two-phase convection, the proper analysis of in-pile experiments calls for an elimination or at least for a sound explanation of the obvious discrepancies. In this context, it has to be mentioned that the influence of non-adiabatic side walls on the onset of convection and the overall heat transfer from particle beds has not been clarified sufficiently. Benocci et al. /90a/ seem to be able to predict reasonably well the onset of convection at reduced Rayleigh numbers and the heat transfer rates observed in the Sandia D-Series in-pile tests /77, 78, 89/ by taking into account non-insulating side walls in their numerical calculations.

Method of Heating	Boundary Conditions	Critical Rayleigh Numbers	Heat Transfer Correlation	Authors
Joule heating	adiabatic lower and isothermal upper boundary	31.8 experimental 32.8 theoretical	$Nu = 0.440 Ra_I^{0.237}$ , $0 < Ra_I < 200$ $Nu = 0.135 Ra_I^{0.553}$ , $200 < Ra_I < 900$	Buretta, Berman /83/
Joule heating	"	33 experimental	$Nu = 0.116 Ra_I^{0.573}$ , $30 < Ra_I < 800$	Sun /82/
Joule heating	"	32. experimental	$Nu = 0.158 Ra_I^{0.5}$ , $30 < Ra_I < 10^4$	Hardee, Nilson /84/
Joule heating	"	36.1 experimental	$Nu = 0.570 Ra_I^{0.35}$ , $40 < Ra_I < 1400$	Kulacki, Freeman /85/
Inductive heating	adiabatic lower boundary and overlying liquid layer	12 experimental	$Nu_p = 0.190 Ra_I^{0.690}$ , *) $Nu_f = 0.234 Ra_f^{0.307}$ , $12 < Ra_I < 3000$	Rhee, Dhir, Catton /86/
Inductive heating	"	15 extrapolated from experiments	$Nu = 0.267 Ra_I^{0.5}$ , $100 < Ra_I < 20000$	Barleon, Werle /87/
Inductive heating	"	30-40 experimental $h_p/b = 2.8$	$Nu = 0.0786 Ra_I^{0.707}$ , $30 < Ra_I < 7500$	Schulenberg, Müller /88/
Inductive heating	"	15 theoretical $h_p/b = 1.0$	$Nu = 0.388 Ra_I^{0.533}$ , $30 < Ra_I < 3000$	Schulenberg, Müller /88/
Nuclear heating	"	0.8 experimental	$Nu = 0.911 Ra_I^{0.34}$ , $0.8 < Ra_I < 14$ $0.57 < h_p/b < 1.56$	Mitchell et al. /78/

\*) see definition of Nusselt number in Table 3.1

Table 3.2 Single phase heat transfer correlations in debris beds.

$g$	acceleration of gravity
$\beta_{\ell}$	coefficient of thermal expansion of liquid
$K$	permeability of the particle bed
$\nu_{\ell}$	cinematic viscosity of liquid
$\kappa$	heat conductivity of the liquid
$\kappa_m$	heat diffusivity of the particle bed (in the mean)
$\lambda$	heat conductivity of the liquid
$\lambda_m$	heat conductivity of the particle bed (in the mean)
$\alpha$	coefficient of heat transfer
$Q$	density of heat source
$q$	heat flux
$T_0 - T_1$	temperature difference between lower and upper side of both layers
$T_M$	temperature at the interface between the two layers
$h_p$	height of particle bed (layer)
$h_{\ell}$	height of liquid layer
$h_p + h_{\ell} = H$	height of combined layers

Table 3.3 Nomenclature of Table 3.2.

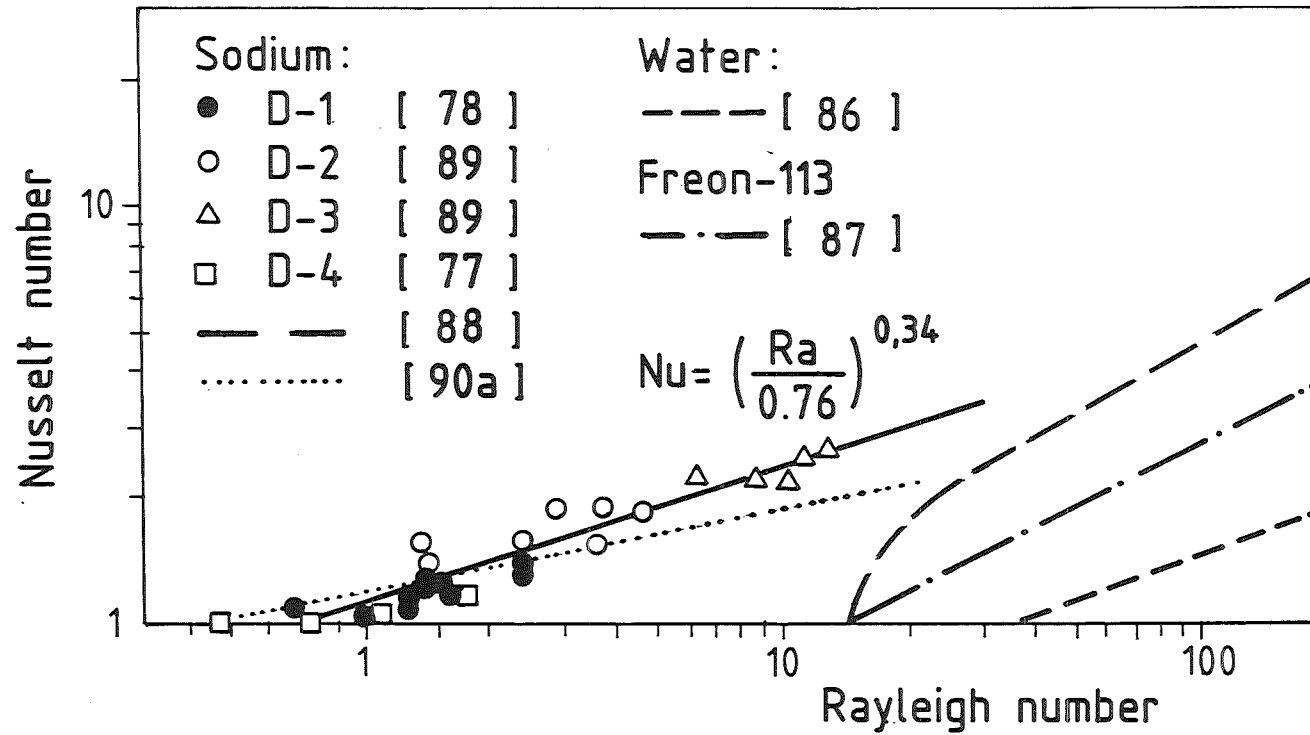


Fig. 9 Overall Nusselt number versus internal Rayleigh number for single phase natural convection in saturated particle layers.

A heat transfer correlation for the more general case of non-isothermal lower and upper boundaries has been derived by Barleon and Werle /87/ following the idea of Baker et al. /91/. The correlation describes the percentage of downward heat flux as a function of the external and internal Rayleigh numbers.

#### 4.53 Boiling Regime

Internal boiling is very efficient in cooling internally heated saturated debris beds. It starts when the temperature in the bed, as a whole or in parts, has reached the saturation temperature of the liquid. Similar to nucleate surface boiling, the mechanism of internal boiling is self-limiting. High steam generation and high steam flow rates prevent the porous body from being replenished by inflowing liquid, and a portion of the bed will become dry. In the dry zones the local bed temperature exceeds the saturation temperature of the liquid. These conditions are considered as limiting conditions for the coolability of debris beds and are usually termed as 'dryout' of the bed. Since the heat transfer from the bed by single-phase steam flow is considerably less than by boiling, the temperature of the bed may reach the melting temperature of the debris. The melting of core debris means a further step of escalation in the course of an accident. Therefore limiting conditions for the bed dryout have been studied both experimentally and theoretically. The investigations are mostly centered around predicting the so called dryout heat flux at the top surface of the debris bed. State of the art reports on this topic have been given before by Squarer et al. /92/, Lipinski /93/ and Buchlin and Benocci /90b/.

These authors cite and evaluate more than 50 relevant contributions to the problems. (Citation on particular aspects of the dryout problem is therefore limited in this section.)

From experimental and theoretical investigations, the following parameters affecting the dryout heat flux have been identified /90b/, /92/, /93/; see also the summary in /5/: a) particle characteristics, i.e. particle size and shape, size and shape distribution, particle density; b) bed geometry, i.e. depth and width of bed; c) bed power density, d) thermal and cinematic conditions at the boundaries of the bed i.e. insulated or cooled bottom, liquid subcooling at top surface, flux of liquid into bed from below or sidewise; e) system pressure; f) fluid thermophysical properties, g) capillary properties, i.e. surface tension, wetting angle, h) structure of bed, i.e. particle stratification, formation of vapor channels or bed loosening by steamflow and flashing disturbances.

Bed dryout has been investigated experimentally by various types of out-of-pile tests and by in-pile tests. In the out-of-pile tests bottom heating and volume heating by either Joule or inductive heating was employed, and the parameter bed depth, bed width and particle diameter were varied typically in the range 5-50 cm, 5-15 cm, and 0.2-15 mm, respectively. The parameter range of the seven Sandia in-pile tests D1-D7 /77-79/, /89/ is limited to a fixed bed diameter of 10 cm, to bed depths varying between 5 and 16 cm and to particle size distributions in the diameter range 0.1-1 mm. The measured dryout heat flux covers the range from 15 kW/m<sup>2</sup> to 4300 kW/m<sup>2</sup>. Most experiments were performed at practically atmospheric pressure. Recently some experimental results for system

pressures up to 0.5 MPa have been reported /213/.

Since the number of in-pile experiments with prototypical materials is limited, model development has been fostered. The models aim at describing consistently all the phenomena observed in the small scale experiments and at transferring the results to reactor conditions. In deriving relations between the dryout heat flux and the influencing quantities listed above, basically two approaches have been employed by the different authors. Balancing mass, momentum and energy of the two phases in the porous body proves to be the best method for describing most of the phenomena simultaneously. Based on this conception, step by step, more sophisticated models have been developed by a refined description of the fluid dynamic interaction between solid particles, liquid and vapor /93/. This generalizing procedure leads to the increasing number of (not always well known empirical) parameters related to the interaction processes. The model relations become cumbersome to handle and finally algebraic correlations have to be replaced by data from numerical computation.

A reduction in the number of different empirical parameters is achieved if, instead of starting from the balance equations, flooding correlations for annular two-phase flow or countercurrent flow in porous bodies are used. A more direct method for obtaining simple expressions for the dryout heat flux is to correlate directly the experimental data by introducing such suitably defined physical quantities as for instance bed loading, superficial vapor velocity based on the power density and the latent heat (see e.g. Ref. /28, 110/).

Some correlations which mark the progress in the model development are compiled in table 4. A detailed compilation and evaluation of the different models has been given in References /90b, 92, 93/.

Based on the great number of experimental and theoretical investigations, it can be stated in general that the physical effects of the majority of the different bed parameters are qualitatively understood and that in particular the problem of the dependence of the dryout heat flux on the particle diameter and the bed depth may be considered as largely settled.

In detail the following phenomena have been observed in experiments or described by physical models:

- The dryout heat flux is independent of bed width /92/.
- In deep beds with small particles the flow is laminar, the ratio of viscosity to bouyancy forces is predicted to depend only on the viscosity ratio, and thus the dryout heat flux increases with the square of particle diameter and is furthermore independent of bed height according to the models in Ref. /84, 94, 95/.
- For shallow beds with small particles, a capillary pressure head in the vapor phase has to be considered, which increases the dryout heat flux with decreasing bed height /98/. In addition vapor channels, flashing disturbances or perhaps fluidization increase the dryout heat flux to a further extend /94, 99, 105/. Models which predict the length of vapor channels are listed in table 4.3.
- In deep beds with coarse particles the flow is turbulent, the ratio of vapor inertia to bouyancy forces depends only on the

Group definitions:

$L = \frac{q_d \nu_g}{K h_{fg} (\rho_f - \rho_g) g}$	<p>dimensionless heat flux for laminar flow model, also ratio of vapor to buoyancy forces,</p>
$T = \frac{q_d^2}{\eta h_{fg}^2 (\rho_f - \rho_g) g \rho_g}$	<p>dimensionless heat flux for turbulent flow model, also ratio of vapor inertia to buoyancy forces,</p>
$C = \sqrt{\frac{\epsilon}{K} \frac{\sigma}{(\rho_f - \rho_g) g H}}$	<p>ratio of surface tension to buoyancy forces,</p>

Nomenclature:

d	particle diameter
g	acceleration of gravity
H	bed height
$h_{fg}$	heat of vaporization
I	Leverett-function
K	permeability
$q_d$	dryout heat flux
S	effective saturation
z	vertical coordinate
$\alpha$	void fraction
$\eta$	passability
$\nu_f, \nu_g$	kinematic viscosity of liquid and gas, resp.
$\mu_f$	viscosity of liquid
$\mu_w$	viscosity of water
$\rho_p, \rho_f, \rho_g$	density of particles, liquid, and gas, resp.
$\sigma$	surface tension
$\theta$	contact angle

Table 4.1 Group definitions and nomenclature of Section 4.53

Applications	Dryout Correlations	Physical Assumptions	Authors
deep beds, small particles	$L = 0.0177 v_g/v_f$	laminar flow, fluid drag only	Dhir, Catton /94/
deep beds, small particles	$L = \frac{1}{[1 + (v_f/v_g)^{1/2}]^2}$	seperated flow, laminar fluid and vapor drag	Hardee, Nilson /84/
deep beds, small particles	$L = \text{Max} \left[ \frac{1-\alpha}{1/\alpha^2 + (v_f/v_g)^{1/(1-\alpha)^2}}, \alpha \neq 1-s^1 \right]$	counter-current annular flow, laminar	Jones et al. /95/
deep beds, coarse particles	$T = 0.0113 \left( \frac{\rho_f}{\rho_g} \right)^{1/4} \left( \frac{\mu_w}{\mu_f} \right)^{0.1}$	flooding model, turbulent flow	Sowa et al. /96a/
deep beds, coarse particles	$T = \frac{0.105}{[1 + (\rho_g/\rho_f)^{1/4}]^4}$	flooding model, turbulent flow	Ostensen, Lipinski /97/
deep or shallow beds, small particles	$L = 0.211 (1 + 0.32 C)$	laminar flow, capillary forces included	Shires, Stevens /98a/
general	$L = \left[ \frac{v_f}{v_g} \frac{1}{S^3} + \frac{1}{(1-S)^3} \right] + T \left[ \frac{\rho_g}{\rho_f} \frac{1}{S^3} + \frac{1}{(1-S)^3} \right]$ $= 1 + C \left( - \frac{dI}{dS} \right) \frac{dS}{d(Z/H)}$	laminar and turbulent flow, capillary forces included	Lipinski /93/

Table 4.2 Dryout correlations for volumetrically heated top fed beds.

1) 'Max' means maximum value of the expression.

Channel length	Authors
$l_c = \frac{6 \sigma}{\epsilon d (\rho_p - \rho_f) g}$	Jones et al. /99/
$l_c = \frac{\sqrt{150} \sigma}{\epsilon d \rho_p g} I(S)$	Schwalm, Nijssing /108/
$l_c = \frac{4.62 \sigma \cos \theta}{\epsilon d (\rho_p - \rho_f) g}$	Reed /109/
$l_c = \frac{\sqrt{150} \sigma \cos \theta}{\epsilon d (\rho_p - \rho_f) g} I(S)$	Lipinski /93/

Table 4.3 Channel length correlations.

density ratio, and the dryout heat flux increases with the square root of particle diameter and is also independent of bed height /96, 97/.

- The downward heat flux from boiling bed regions to a cooled bottom plate is enhanced by capillary forces, a mechanism similar to that of heat pipes /93, 100, 104/.
- The dryout heat flux is considerably increased if liquid can penetrate from below (bottom fed beds) /98b, 101/.
- The dryout heat flux decreases with decreasing bed porosity and with increasing standard deviations of the particle size distribution /92/.
- The dryout heat flux is reduced in stratified particle beds with the smaller particles in the upper zone compared to the one in a homogeneous bed composed of the smaller particles /78, 79, 93, 105, 106/.
- Subcooling a liquid layer on top of particle beds enhances, on one side, the dryout heat flux by reducing the effective bed depth and by stimulating single-phase convection heat transfer /84/. On the other side, subcooling, delays or even suppresses the formation of vapor channels /77, 104, 107/ and therefore reduces the overall value of the dryout heat flux.
- The dryout heat flux is increased if the system pressure increases /92, 213/.

In figures 10 and 11, some typical results are displayed. Figure 10 shows a comparison between experimental results obtained by out-of-pile tests with simulant materials and theoretical predictions of the dryout heat flux as a function of the particle diameter and the bed height. For the whole range of test data the experimental results are predicted well by the theoretical model of Lipinski /93/. The other theoretical curves show reasonable agreement with the test data only in subranges, since in each case only part of the physical effects are modeled.

In figure 11, results from in-pile and out-of-pile Sodium-UO<sub>2</sub> experiments are displayed. The data points of the in-pile experiments demonstrate that the 'reference' values for the dryout heat flux obtained from fresh homogeneous particle beds are reduced by about a factor one half in the case of bed stratification and can get enhanced considerably by disturbances (e.g. vapor channels) in the packing of the bed. Differences exist between the out-of-pile data and the 'reference' in-pile-data. These differences can not be explained satisfactorily to date. The model of Lipinski for packed bed predicts reasonably well the 'reference' in-pile data. The extended Lipinski model taking into account channeling effects seems to cover also the physical effects of bed disturbances. However, uncertainties exist with respect to the latter point since bed disturbances may have other characteristics than vapor channels.

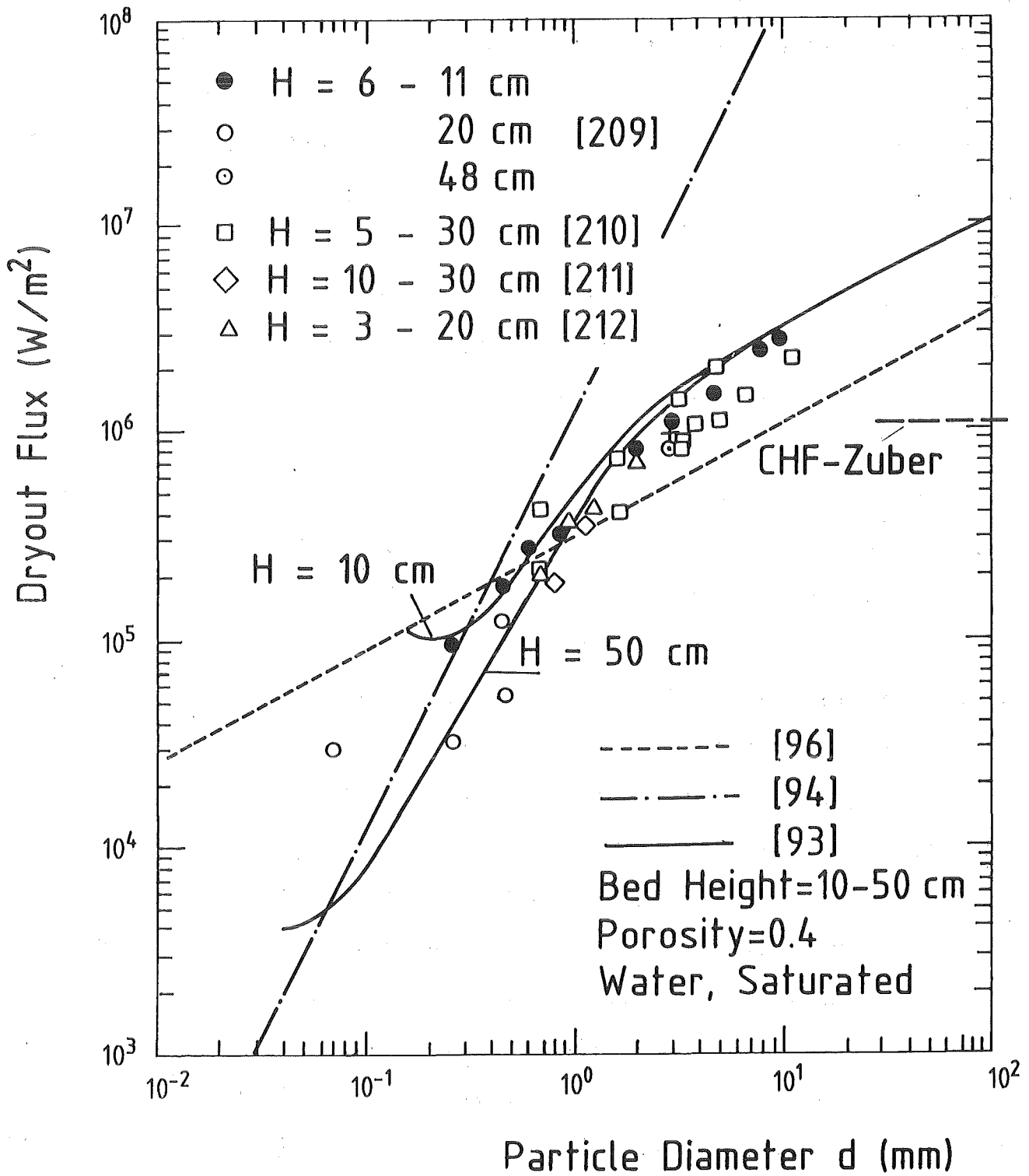


Fig. 10 Dryout heat flux as a function of particle diameter.

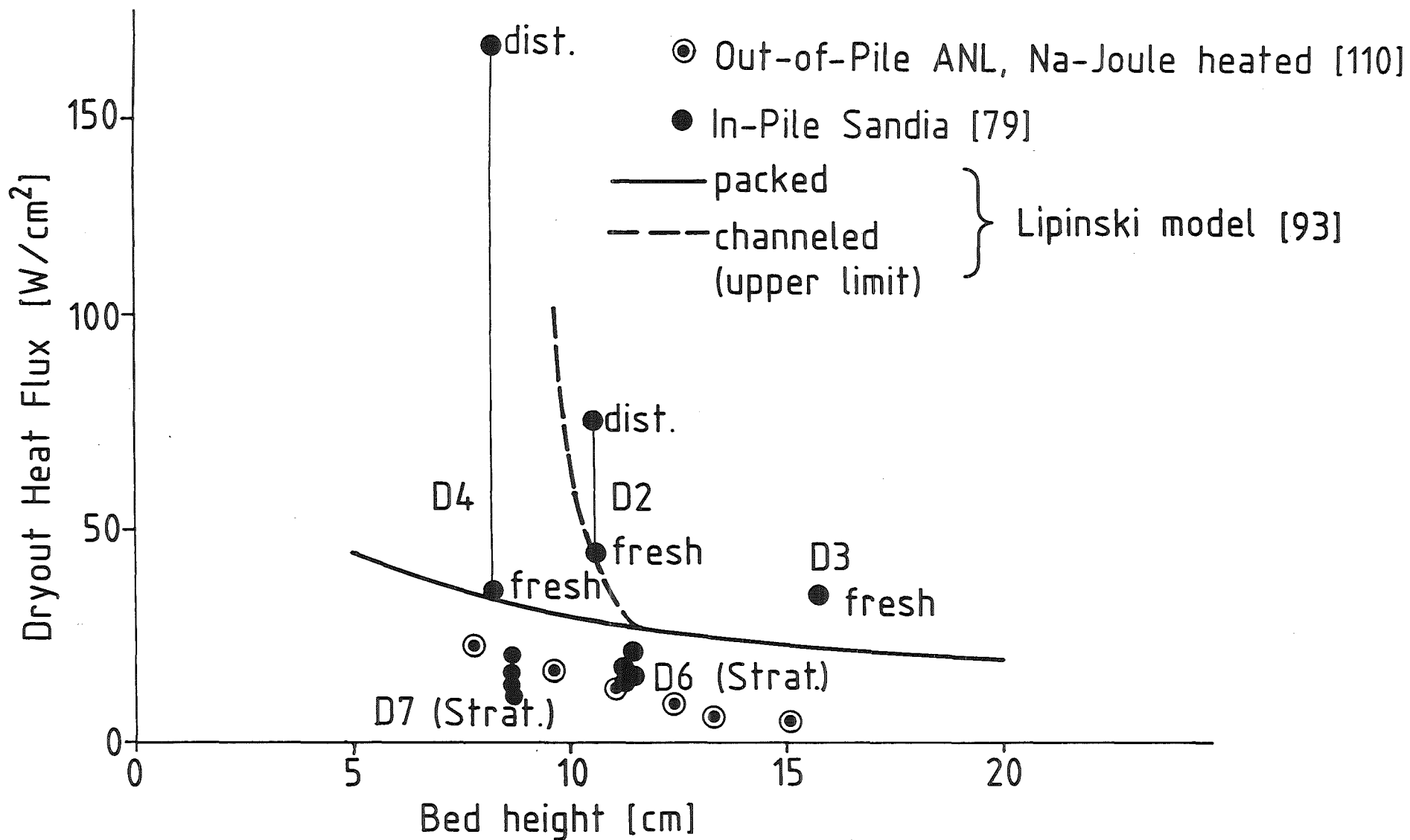


Fig. 11 Dryout heat flux versus bed height for in-pile and out-of-pile experiments with  $UO_2$ -particles and sodium as a coolant. Particle size: range 0.1-1 mm.

As far as the in-vessel coolability of core debris in case of LMFBR's is concerned, further investigations should concentrate on the better understanding and prediction of the mechanism of subcooling in connection with vapor channel formation and the dynamic restructuring of the bed by flashing events.

Further experiments with large bed heights, typically in the order of meters and at elevated system pressures, are required for confirming the available models which are to be used for predicting the coolability of degraded LWR cores.

According to the specific features of LWR severe core damage accidents, it is also of some interest to understand the reentry of coolant into high temperature debris beds and to assess the rate of vapor generation by the quenching process. Only a limited number of experiments have been performed addressing the quenching of a hot debris bed /102b, 103/. The preliminary experiments employing slender cylindrical debris columns indicate that the quench front propagation is affected by three-dimensional effects.

In summary it can be stated that in comparison to other PAHR topics the knowledge of single- and two-phase cooling of debris beds is well advanced. Nevertheless, some uncertainties concerning particular details need further clarification.

#### 4.5.4 Post Dryout Heat Transfer

It may be conjectured that there is a considerable potential for removing heat from dry core debris beds by conduction, radiation and gas convection, before extended melting of the particle bed occurs. Although this question has not been treated systematically, the first five screening in-pile tests (MP-1, MP-2, MP-3S, MP-4, MP-5S) of the Molten Pool Series at Sandia /111-114/ are elucidating the phenomena to be expected in a dry fuel or fuel-steel particle bed in the temperature range between 3000 K and 3140 K.

From post-test x-ray and metallographic examinations of the debris containing capsule and from temperature histories, the following facts were stated /111/: a) There was no indication of sintering in pure  $UO_2$  particle beds (particle sizes in the range 0.1 to 1 mm) at locations surrounding the zone of incipient melting. b) In particle beds consisting of a mixture of  $UO_2$  and steel particles, significant migration and agglomeration of molten steel occurred from the hottest into cooler zones of the bed. This migration caused the formation of a void, surrounded by crusted debris. A schematic drawing of the radiograph of the MP-5S test is given in figure 12.

It is still unclear under which conditions sintering of an  $UO_2$  particle bed can occur. Sintering has been observed in out-of-pile experiments employing furnace heating /112/. Sintering is believed to deteriorate cooling conditions of debris beds in general by reducing the porosity and by preventing channeling and bed leveling. Therefore a better understanding of this phenomenon is needed. However, further investigations should take into account the effect of sodium either as liquid or vapor.

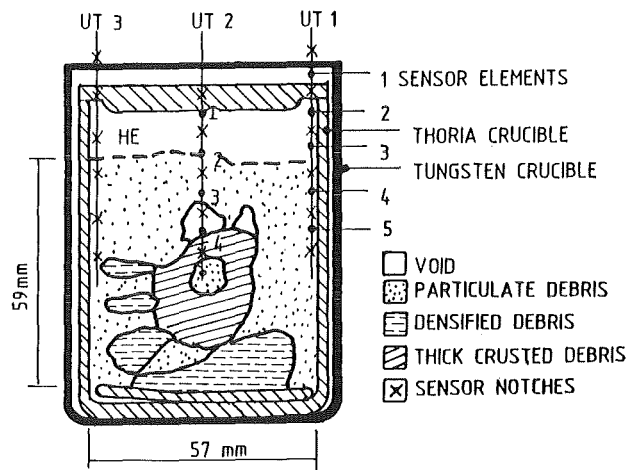


Fig. 12 Schematic drawing of the MP-5S bed of the Sandia in-pile experiment /114/.

It has been proposed by Plain et al. /114/ that the migration of molten steel in the  $UO_2$  particle bed is due to the effect of capillary forces and temperature gradients. The generation of crusts and cavities is expected to change largely the thermal characteristics and the direction of heat fluxes by inducing strong inhomogeneities in the porous body. Our current lack of knowledge for the Post Dryout Phase was schematically summarized by Kayser and Rigoleur /115/ and is displayed in figure 13.

Since neither the migration process nor the processes of melting, of cavity and of crust formation as well as the relevant question of crust stability is physically well understood, the potential of post dryout heat transfer can not be fully exploited for accident analysis. More experimental and theoretical research work is needed in support of the in-pile experiments to clarify the preliminary observations. The European PAHR in-pile Program in progress is particularly aimed at providing the necessary information of the post-dryout behavior of debris particle beds /116/.

#### 4.6 Heat Transfer from Molten Layers

##### 4.6.1 Single-Phase Convection

Debris beds can turn into molten pools if the heat transfer from the porous bed is limited and the temperature inside the bed exceeds the melting point. Based on observations in small scale melting experiments with mixtures of  $UO_2$  and steel particles /117, 118/, it is anticipated that steel and fuel, i.e. the metallic and the oxidic phase segregate due to their density differences, so that two separate layers develop.

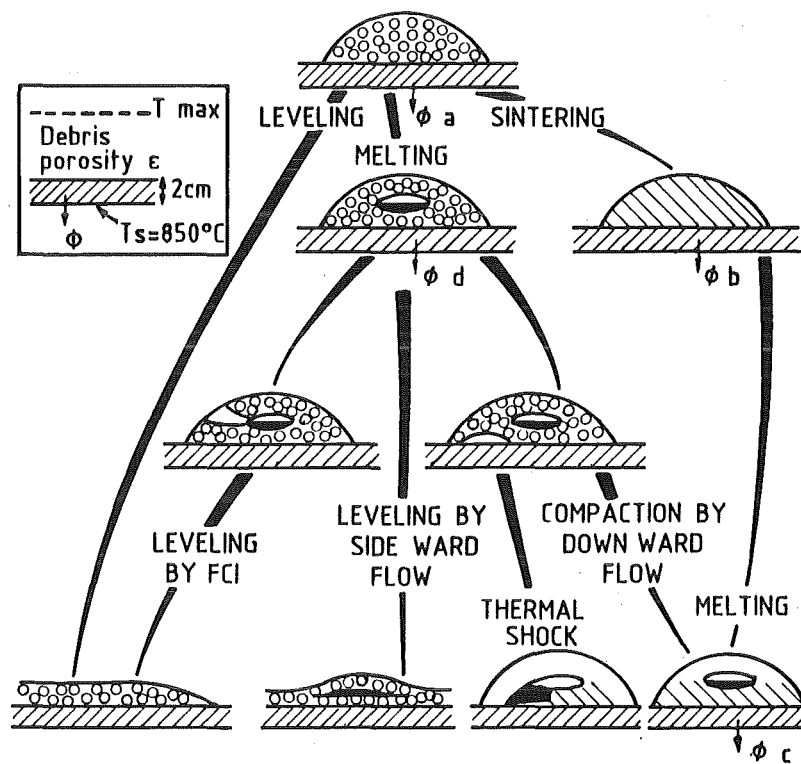


Fig. 13 Evolution of a particle debris pile, schematically after Kayser and Le Rigoleur /115/.

Heat transfer by single phase natural convection from horizontal fluid layers with volumetric energy sources has been extensively studied in the past for various geometries and different thermal boundary conditions. Correlations for the heat transfer have been obtained from direct numerical simulation /119-125/, i.e. by integrating the balance equations of mass-, momentum and energy employing finite difference schemes and from experiments by employing Joule heating in simulant liquids /126-130/. Chung et al./131b,132a,b/ have derived correlations for turbulent thermal convection at very high Rayleigh numbers analytically employing a boundary layer approach and asymptotic analysis. This procedure validates the functional dependence of the available numerical and experimental results, and moreover guarantees an extrapolation of the heat transfer relations beyond the range covered by experimental results.

The influence of different geometrical shapes on the partition of the upward, downward and sideward heat fluxes has received also some attention in references /120, 124, 131a, 133a/. The investigations have generally shown that the convective heat flux to the lateral walls is of the same order as the upward heat flux. In particular the hottest zone at the sidewalls occurs close to the top surface of the layer<sup>1)</sup>. Without claiming completeness, some data and correlations for different geometrical forms are compiled in table 5 together with the definitions of the relevant groups. A review of this particular topic has been given before by Baker et al. /91/.

1) Mixing processes other than by natural convection e.g. by dropping molten material into the pool can remove the hottest zone at the side walls to other positions /120b/.

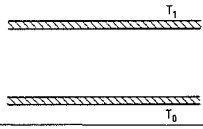
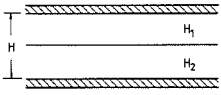
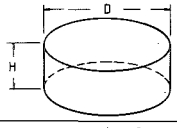
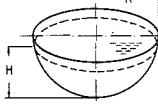
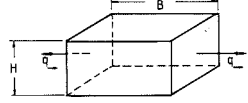
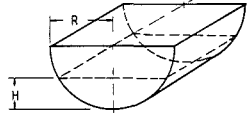
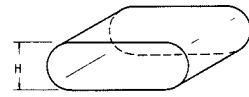
Geometry	Boundary Conditions	Correlation and Range of Application	Definitions	Ref.		
 <p>Infinite Horizontal Plates</p>	adiabatic lower, isothermal upper plate isothermal plates, equal temperature isothermal plates, unequal temperatures	$Nu_{\uparrow} = 0.396 Ra_{\uparrow}^{0.227}, Nu_{\downarrow} = 0$ $Nu_{\uparrow} = 0.342 Ra_{\uparrow}^{0.23} Pr^{0.085}$ $Nu_{\downarrow} = 1.324 Ra_{\downarrow}^{0.10} Pr^{0.085}$ $(1 - \eta)^{0.870} (\eta^2 - Ra_{\downarrow} / Ra_{\uparrow})^{-1} = 0.202 Ra_{\uparrow}^{0.226}, \eta = Nu_{\uparrow} / (Nu_{\uparrow} + Nu_{\downarrow})$	$Nu = \frac{h H}{\lambda}$ $Ra_{\uparrow} = \frac{g \beta H^3}{\kappa \nu} \frac{Q}{2 \lambda}$ $Ra_{\downarrow} = \frac{g \beta H^3}{\kappa \nu} (T_1 - T_0), \eta = \frac{q}{Q H}$	[126] [120] [91]		
 <p>Infinite stratified Layer</p>	isothermal plates, unequal temperatures lighter liquid on top, Heat sources in either one or both layers	$\eta_{\uparrow} (Ra_{\uparrow}^{H_1}), Ra_{\uparrow}^{(H_1)}, Ra_{\uparrow}^{(H_2)}$ $10^4 \leq Ra_{\uparrow} \leq 10^9$		[122]		
 <p>vertical Cylinder</p>	isothermal walls, temperature at bottom equal to temperature at side walls	$Nu_{\uparrow} = 0.748 Ra_{\uparrow}^{0.127}$ $Nu_{\uparrow} = 0.706 Ra_{\uparrow}^{0.184}$ $Nu_{\downarrow} = 0.195 Ra_{\downarrow}^{0.222}$ $Da = 1.67 Ra_{\downarrow}^{0.206}$ $H/D = 1, 10^9 \leq Ra_{\uparrow} \leq 2 \cdot 10^{12}$	$Nu_{\uparrow} = 1.12 Ra_{\uparrow}^{0.103}$ $Nu_{\uparrow} = 0.414 Ra_{\uparrow}^{0.216}$ $Nu_{\downarrow} = 0.163 Ra_{\downarrow}^{0.244}$ $Da = 0.985 Ra_{\downarrow}^{0.207}$ $H/D = 0.25, 10^7 \leq Ra_{\uparrow} \leq 4 \cdot 10^9$	$Da = \frac{Q H^2}{\lambda (T_0 - T_1)} = Nu_{\uparrow} + Nu_{\downarrow} + 4 \frac{H}{D} Nu_{\downarrow}$ $Ra_{\uparrow} = \frac{\beta g Q H^5}{\nu \lambda \kappa}$	[133a]	
 <p>spherical Shell</p>	1. free surface to atmosphere, isothermal wall, 2. isothermal, no slip walls	$Nu = 0.55 Ra_{\uparrow}^{0.15} (H/R)^{1.1}$ $Nu_{\uparrow} = 0.40 Ra_{\uparrow}^{0.2}, Da = 2.25 Ra_{\uparrow}^{0.2}$ $Nu_{\downarrow} = 0.55 Ra_{\downarrow}^{0.2}, H/R = 1$	$0.5 \leq H/R \leq 1.0$ $2 \cdot 10^{10} \leq Ra_{\uparrow} \leq 2 \cdot 10^{11}$ $10^{10} \leq Ra_{\downarrow} \leq 10^{16}$	$Pr = 7$ $Pr = 0.5$	$Nu = \frac{h R}{\lambda}, Ra_{\uparrow} = \frac{g \beta Q R^5}{\kappa \nu \lambda}$ $Da = \frac{Q R^2}{\lambda (T_{max} - T_1)}$	[134] [120]
 <p>rectangular cavity</p>	four isothermal walls, two adiabatic side walls	$Nu_{\uparrow} = 0.345 Ra_{\uparrow}^{0.233}$ $Nu_{\downarrow} = 0.6 Ra_{\downarrow}^{0.19}$ $Nu_{\uparrow} = 1.389 Ra_{\uparrow}^{0.095}$ $Da = (1.05 + 1.2 H/B) Ra_{\downarrow}^{0.19}$ $\eta_{\downarrow} (Ra_{\downarrow}, Ra_{\uparrow}), \eta_{\uparrow} (Ra_{\downarrow}, Ra_{\uparrow})$	$10^6 < Ra_{\uparrow} < 3 \cdot 10^{10}$	$Pr = 7, H/B = 1/2$	$Ra_{\uparrow} = \frac{g \beta Q H^5}{\kappa \nu \lambda}$ $\eta_{\downarrow} = \frac{q_{\downarrow}}{Q H}, \eta_{\uparrow} = \frac{q_{\uparrow}}{Q H}$	[120] [137]
 <p>infinite semicircular cylinder</p>	isothermal, no slip walls,	$Nu_{\uparrow} = 0.36 Ra_{\uparrow}^{0.23}$ $Nu_{\uparrow} = 0.54 Ra_{\uparrow}^{0.18} (H/R)^{0.26}$ $Da = 1.6 Ra_{\downarrow}^{0.2}$ $Nu_{\downarrow} = 0.38 Ra_{\downarrow}^{0.16}$ $Nu_{\uparrow} = 5.34 Ra_{\uparrow}^{0.068}$	$10^7 \leq Ra_{\uparrow} \leq 5 \cdot 10^{10}$ $0.3 \leq H/R \leq 1$	$Pr = 7$	$Ra_{\uparrow} = \frac{g \beta Q H^5}{\kappa \nu \lambda}$ $Nu_{\downarrow} = \frac{Q H}{\lambda (T_{max} - T_1)}$	[120] [133b]
 <p>slab with two side walls of cylindrical shape</p>	upper wall and flat lateral walls nearly adiabatic, lower wall and curved side walls isothermal	$Nu_{\downarrow} = 0.7 Ra_{\downarrow}^{0.2}$	$2 \cdot 10^{11} < Ra_{\downarrow} < 4 \cdot 10^{12}$	$Pr = 7$	$Ra_{\downarrow} = \frac{g \beta Q H^5}{\kappa \nu \lambda}$	[133b]

Table 5 Heat transfer from volume-heated pools;

$Nu_{\uparrow}$  - upward Nusselt number,  $Nu_{\downarrow}$  - horizontal Nusselt number,  $Nu_{\downarrow}$  - downward Nusselt number.

In spite of the many experimental investigations with simulant liquids, there is still an unexplained experimental finding concerning the downward heat flux from a molten  $UO_2$  pool generated by Joule heating from a  $UO_2$  particle bed. In repeated experiments, Stein et al. /135, 136/ measured downward heat fluxes, which were larger by a factor of 2.5 to 4.5 compared to the predictions based on the correlations for natural convection. The experiments were, however, unlike the ones with simulant materials, characterized by strong insulating effects of a large gas-filled cavity between the upper free surface of the pool and an  $UO_2$  crust on top of the experimental arrangement. It has been proposed by several authors /137-142/, that radiative heat transfer in a transparent  $UO_2$  melt may largely contribute to the overall heat transfer in molten  $UO_2$  layers. However, this idea must be questioned on the bases of the experimental results by Bober et al. /143/ that molten  $UO_2$  is practically opaque for thermal radiation up to temperatures exceeding 4000 K (see table 10 in the appendix and the related literature).

The remaining uncertainty should be eliminated by additional analysis and out-of-pile investigations before molten pool in-pile experiments are performed.

#### 4.6.2 Heat Transfer from Boiling and Bubbling Pools.

If the temperature in the molten pool of core debris exceeds the boiling temperature of one or more of the metallic or oxidic components, vaporization and thus pool boiling sets in.

Although heat removal from a boiling pool to the surrounding boundaries applies more to the problem of subassembly failure propagation

during the so called Transition Phase of a core melt down accident than to the quasi-stationary PAHR Phase, it is briefly discussed here for the reason of completeness of the topic.

For single-component fluids, the onset of boiling is determined from a Damköhler-Rayleigh number relation which has been derived from experimental data /120, 121, 129, 133a/.

The heat transfer to the lateral boundaries of a molten pool has been investigated experimentally employing Joule heating or microwave heating of simulant fluids. The experimental findings can be correlated well by assuming that a downward boundary-layer flow at the lateral sidewalls is essentially driven by the updraft of the vapor bubbles in the bulk of the pool. The relevant dynamic group, the Rayleigh number, is therefore based on the overall void coefficient  $\alpha$  of the boiling pool. Correlations for laminar and turbulent convective heat transfer to vertical and horizontal walls and also for the void distribution in the pool have been set up /144-149/. These correlations rely mainly on experimental measurements. Some correlations for boiling pool heat transfer are compiled in table 6.

With respect to transferring the phenomena and correlations to accident conditions, two major deficiencies exist. The experimental investigations have not taken into account boiling phenomena in two- or multi-component fluid systems, as they are expected to occur in molten pools of core debris. Moreover, if for the reason of extreme experimental difficulties (i.e. high temperatures and compatibility of crucible and melt materials) fuel and steel have to be ruled out, more realistic simulant liquids than aqueous salt solutions should be used to scrutinize existing results in an intermediate step.

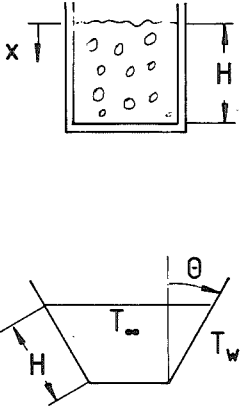
Geometrie	Boundary Conditions	Correlation and Range of Application	Definitions	Ref.
	<p>isothermal side walls and bottom,</p>	<p><math>Nu_{\rightarrow} = 1.54 Ra^*^{0.25}</math>, <math>Ra^* &lt; 2 \cdot 10^{11}</math> laminar bubbly flow</p> <p><math>Nu_{\rightarrow} = 0.0309 Ra^*^{0.40}</math>, <math>Ra^* &gt; 2 \cdot 10^{11}</math> turbulent bubbly flow</p> <p><math>0.2 &lt; j_{g\infty}/u_{\infty}</math> bubbly flow regime</p> <hr/> <p><math>Nu_{x_{\rightarrow}} = 0.16 Ra_p^{1/3}</math> <math>3 \cdot 10^9 &lt; Ra_p &lt; 3 \cdot 10^{12}</math></p> <p><math>Nu_{\rightarrow} = 3.8 Nu_{\downarrow}</math> <math>q &gt; 8.37 \text{ W cm}^{-2}</math></p> <p><math>Nu_{\rightarrow} = 3.10 Re^{1/2}</math> <math>2.8 &lt; Pr &lt; 4</math> <math>2 \cdot 10^3 &lt; Re &lt; 2 \cdot 10^5</math></p>	<p><math>Ra^* = \frac{g\alpha H^3}{\nu_f^2} \cdot Pr_f \cos \theta</math></p> <p><math>Nu = \frac{h H}{\lambda_f}</math> <math>Nu_x = \frac{h x}{\lambda_f}</math></p> <p><math>Ra_p = (\beta_f(T_{\infty} - T_w) + 3\alpha) \frac{g x^3}{\nu_f^2} \cos \theta \cdot Pr \cdot [1 + (\frac{0.492}{Pr})^{9/16}]^{-16/9}</math></p> <p><math>Re = \frac{H \cdot j_{g\infty} \rho_f}{\mu_f}</math></p> <p><math>h^*</math> heat transfer coefficient after Haberstroh and Reinders [157]</p>	<p>[146]</p> <hr/> <p>[147]</p> <hr/> <p>[144]</p>
	<p>interfacial heat transfer between superimposed immiscible liquids</p>	<p><math>q = h h^* \Delta T^{4/3}</math></p> <p><math>h = 1 + 608 \cdot \frac{j_{g\infty}}{u_{\infty}} \left( \frac{\rho_h - \rho_l}{\rho_l} \right)^{-0.43}</math></p> <p><math>0 &lt; j_{g\infty} &lt; 0.4</math> oil-water</p> <p><math>0 &lt; j_{g\infty} &lt; 0.6</math> water-woods metal</p>	<p><math>j_{g\infty}</math> superficial gas velocity</p> <p><math>u_{\infty}</math> terminal rise velocity of bubbles</p> <p><math>\alpha</math> void</p>	<p>[153]</p>

Table 6 Heat transfer from boiling and bubbling pools.

Similar phenomena like in boiling pools are found in gas bubbling molten pools, where the gas is released into the pool from the disintegrating boundaries. Such a situation may occur if a core melt interacts with gas generating sacrificial material e.g. concrete. Compared to single-phase convection the downward heat transfer from the molten, gas agitated pool to the lower wall is largely increased by the vigorous stirring effect of the perculating bubbles. The heat transfer rates are described in this case by models similar to those for nucleate or film boiling on heated flat surfaces in which, however, heat transfer by radiation through the gas phase is included. These models have been developed on the basis of observations from small scale laboratory experiments with simulant materials, for instance by employing frozen benzene globules embedded in dry ice for simulating the concrete slab and heated water pools for simulating the core melt /150, 151/ (see also section 4.7). Verification of the heat transfer models by medium scaled experiments employing several hundreds of kg's of molten steel and ceramic material at temperatures of the order of 2000 K is under way within the BETA Test Program at the Kernforschungszentrum Karlsruhe /152/.

Compared to single-phase convection, the heat transfer is largely enhanced at the interface of superimposed liquid layers when it is penetrated by a stream of gas bubbles. Corresponding relations between the heat flux and the gas flow rates have been established from experimental data /153-156/. The relations correspond to those of Haberstroh and Reinders /157/ for single-phase heat transfer at an interface of two overlying liquids. In the experiments, gas was injected through a porous bottom plate into a pool consisting of two

superimposed immiscible liquids. Heat was added to the experimental apparatus either by heating the bottom plate /153m 154/ or by Joule heating of the lower of the two liquid layers /155/. Two typical regimes of heat transfer have been identified. The first is characterized by a high density ratio of the heavier to the lighter liquid and moderate superficial gas velocities resulting in an interfacial agitation without perceptible entrainment effects. The second mode occurs when the density ratio is close to one and/or the superficial gas velocities are high. In this case, considerable entrainment of droplets of the heavier liquid into the lighter fluid is observed resulting in thick mixing layers at the interface. The influence of entrainment and mixing on the increased interfacial heat transfer is not completely understood and model development needs improvement.

#### 4.7 Molten Pool Penetration into Substrates

If the contact temperature between core melt and substrate exceeds the melting temperature of the substrate, the molten pool will expand beyond its initial geometry. For assessing in this case the retention capability of reactor structures or special retention devices for core debris, the propagation of the melt front must be predicted. Since the melt front propagation can be directly related to the local heat fluxes at the wall-melt interface, the problem is reduced to the determination of the heat flux towards the rigid walls. Depending on the relevant wall material e.g. magnesia, alumina, concrete, the heat flux from the molten pool to the surrounding walls is strongly influenced by the mixing characteristics

between the molten core debris and the molten wall material, i.e. by the interfacial mass transport. Current research work concerning melt front propagation can be ordered by three aspects: a) the molten core debris mixes completely with the molten wall material (mutual dissolution), b) the core melt and the molten substrate is immiscible, c) the wall heat flux is determined by a gas stream resulting from a thermal decomposition of the wall material, which in particular is concrete.

From experimental studies using simulant and prototypical materials mainly the following factors have been found to influence the growth rate of molten pools in cases a) and b).

The relative rates of sideward and downward growth are mainly determined by the bulk temperatures of the pool and the melting temperature of the walls, the density ratio of the pool and the molten or decomposed wall material. Furthermore the viscosity of the pool liquid and, in case b) of immiscible materials, the surface tension between pool and molten substrate have also a distinct influence. In the high temperature phase, where solidification and crust formation at the pool-wall interface can be excluded, downward propagation of the melt front predominates if the pool density is larger by a factor of about 1.1 compared to the molten wall material [164, 166]. This effect is due to the agitation of the lighter molten wall material rising within the thermal conduction layer of the pool in turn forcing hotter pool material downward towards the cooler wall. In a phase with reduced pool temperatures, or for density ratios near 1, the sideward growth of the pool becomes predominant. In this case agitation of the pool by a

multi-component flow is suppressed by crust formation or reduced buoyancy of the molten wall material and the heat flux and therewith the melting rate at the boundaries are mainly regulated by conduction and free convection like in molten pools. As it was discussed in section 4.61 the sideward heat flux from molten pools with internal heat sources is considerably larger than the one in downward direction.

This general picture was first outlined by Faw and Baker /158/ who employed in their experiments mutually soluble simulant material, i.e. inductively heated salt solutions and substrates of carbomax. Their results were confirmed by Fieg and Werle /159/, who used similar experimental techniques.

From the different experimental investigations employing mutual soluble and immiscible materials one can learn moreover that the dissolution process by diffusion only does practically not influence the propagation of the melt front. Only if mixing is enhanced by some strong stirring process, e.g. by gas bubble percolation in the pool, mutual solubility between the different materials increases the growth rate of the molten pool.

Another most evident general property for molten pool growth was communicated by Turland et al. /162/: Advancing melting fronts are stable to local perturbations i.e. deepenings, corners, and protrusions on the confining walls are smoothed out by the advancing melt front.

Besides these generally agreed statements reliable correlations for the wall heat flux are available only for a few cases. In particular

their validity and range of application is not or not well enough confirmed to be finally usable as predictive tools for core melt propagation into structures. These more specific results are outlined next.

For the downward heat transfer in a miscible melting system Farhadieh and Baker /164, 165/ have derived correlations from experiments with externally and internally heated pools. They identified four different hydrodynamic flow regimes occurring in different ranges of the density ratio  $g^*$  of the pool and the molten wall material, namely a range of diffusive mixing and heat conduction for  $g^*$  close to one, a range of transition to turbulent mixing and heat transfer and regimes of moderately turbulent and highly turbulent mixing and heat transfer for  $g^* > 1.1$ . The proposed correlations are compiled in table 7. Employing similar techniques like Farhadieh in his experiments, Eck /166/ confirms the existence of the different flow regimes, but finds downward heat fluxes generally smaller by a factor of one third. Eck gives a critical assessment of these and other deficiencies in the measured heat flux, obtained from miscible melting systems consisting of simulant materials.

A correlation for the sideward melting rate has been derived by Chen and Baker /167/. They claim that the predictions of their model are within a few percent of the experimental melting rates given in reference /168/. No confirmation of these results is available from other research groups.

System Characteristics	Correlations	Definitions	Ref.
Miscible Melting System	$Nu_i \frac{Pr_l}{Pr_m} = 1.75 \cdot 10^{-5} Ra^{1.19}$ $10^{-1} < Ra < 10^4$ $2.8 < Pr_l < 400$ $13.6 < Pr_m < 2000$ $0.7 < \rho_l / \rho_m < 50$	$Ra = \frac{g (\rho_e - \rho_m) \Lambda^3}{\nu_m \kappa_m}$ $\Lambda = \frac{\mu_l^{3/2}}{(\rho_l - \rho_m)^{3/2} g^{1/3}}$ $Nu_i = \frac{\Lambda \rho_m h_m}{\Delta T \lambda_m}$	[165]
Miscible or Immiscible System	$Nu_{-} = \left( \frac{1}{\sqrt{2}} \frac{h_{ms}}{c_{pm} \Delta T} \frac{\Delta \rho g L^3}{\rho_m \nu_m \kappa_m} \right) \zeta^{3/4} \left( \frac{x}{L} \right)^{-1/4}$ $\zeta^{1/2} / (1 - \zeta) = \left( \frac{3}{\pi} \frac{\lambda_l \rho_l c_{pl} \Delta T}{\lambda_m \rho_m h_{ms}} \right)^{1/3}, \quad Pr_l \gg 1$ $Sc \gg Pr_m$	$Nu_{-} = V_m \frac{\rho_s h_{ms} L}{\lambda_m \Delta T}$ $V_m = \text{melting rate}$ $\zeta = \frac{\Delta T_m}{\Delta T}$	[167]
Immiscible System	$Nu_i = 0.627 Ra^{1/5}$ $10^4 < Ra < 10^7$	$Nu_i = \frac{q \Lambda}{\lambda_m \Delta T}$ $Ra = \frac{\rho_m h_m g (\rho_l - \rho_m) \Lambda^3}{\mu_m \kappa_m \Delta T}$	[170a]
Immiscible System	$Nu_i = 0.20 Ra^{1/4}$ $\Delta T > 20 \text{ K}$	$Ra = \frac{\rho_m h_{ms} g (\rho_l - \rho_m) \Lambda^3}{\mu_m \kappa_m \Delta T}$ $Nu_i = \frac{q \Lambda}{\lambda_m \Delta T}$ $\Lambda = [\sigma / g (\rho_l - \rho_m)]^{1/2}$	[169]
Gas Releasing System, bubbly flow	$\frac{q}{\Delta T} = 0.4487 V_{sg}^{0.396} \text{ W/cm}^2 \quad (\text{Air/Water})$	$V_{sg} - \text{superficial gas velocity}$	[170b]
film boiling	$Nu_i = 0.44 \left[ \frac{Gr Ste Pr_g}{x_g} \right]^{1/4}, \quad Gr = g \frac{\Delta \rho}{\rho} \frac{\delta^3}{\nu_g^2}$ $Nu_i = \frac{q \delta}{\lambda_g \Delta T}, \quad Ste Pr_g = \frac{\mu_g h_g}{\lambda_g \Delta T}$	$\delta = [\sigma / g (\rho_l - \rho_g)]^{1/2}$	[151]

Table 7.1 Heat transfer correlations corresponding to molten pool penetration into substrates.

Nomenclature:

$h_m$  latent heat of melt  
 $h_{ms} = h_m + c_{ps} \Delta T$   $H'_{ms} = h_m + \frac{1}{2} c_{ps} \Delta T$   
 $\Delta T$  difference between bulk temperature and wall  
 $\Delta T_m$  temperature difference across the melt layer  
 $q = \rho_m h_m V_m$  melting heat flux  
 $V_m$  melting rate

Indices:

m melt  
l liquid (pool)  
s solid (wall)  
g gas

Table 7.2 Nomenclature of Table 7.1

The situation is similar for immiscible melting systems with liquid components only. Taghavi-Tafreshi et al. /169/ as well as Farhadieh et al. /170a/ and Schramm /171/ find from their experiments and theoretical considerations that the downward heat flux depends strongly on the density ratio of pool and molten wall material and on the surface tension. Differences exist in the functional dependence of their heat transfer correlations. These are, however, less pronounced than in the previous case. No experimentally confirmed general transfer correlations for the heat flux at vertical melting walls in such an immiscible system is known. Preliminary results for predicting the sideward heat flux have been obtained by Beyer and Alsmeyer /172/. These results show, that the natural convection heat transfer can be strongly enhanced by the gravity induced flow of the melt film along the sidewalls.

Felde et al. /160/ have extended the investigations concerning case a) and case b) to volumetrically heated pools penetrating into miscible gas releasing substrates (case c)). In their experiments, they observe that initially the pool depth increased at a faster rate than its width. This trend was reversed later during their experiments. The turn-around time depended on the power density, the density ratio and the gas release rate, which changed due to dissolution.

Farhadieh /173a/ reports that, even at very low gas release rates, an enhanced downward heat transfer is observed due to gas agitated convective mixing near the wall. However, it is yet unclear, to what extent and in which range buoyancy effects due to density differences

of the liquid constituents and gas bubble driven agitation interact and determine the wall heat flux and the melting rates.

An increased lateral progression of a gas agitated heated pool was found also by Alsmeyer /161/ when he lowered the bulk temperature of the pool in such a way that solid crusts formed at the lower pool side, thereby inhibiting the perculating gas flow. In his experiments Alsmeyer employed parafin oil of high viscosity filled into a cavity of dry ice of dimension height/width/depth as 40/40/30 (cm) and heated at different power levels by a heater coil.

A comparatively clearer picture for the heat transfer on vertical and horizontal boundaries emerges if the gas release rates of the decomposing wall constituents are very high (superficial gas velocities larger than  $1 \text{ cm s}^{-1}$ ). Such a situation is typically realized during the high temperature phase of interaction of core melt and concrete. As was pointed out in section 4.6.2, the melt front propagation in downward and lateral direction is determined by heat transfer correlations equivalent to those for film or nucleate boiling and are therefore usually termed as gas film and discrete bubble model /151, 173a/. These models have been confirmed in small scale separate effect tests /171, 174-177/. A final assessment of their applicability to long term core melt concrete interaction is in progress /152/.

#### 4.8 Response of Special Barrier Materials to Hot Debris

If the reactor vessel fails during a core melt down accident, the core debris and the coolant will be discharged into the lower reactor cavern and interact with the concrete structure of the basemat or with the liner material of an ex-vessel core catcher.

In order to prevent unexceptable consequences, the final barrier for the core debris should combine the following desirable characteristics: a) The propagation of the debris has to be stopped or at least effectively delayed. b) The average temperature of the debris has to be reduced as fast as possible by melting the sacrificial material and mixing with it. c) The release of fission products from the core debris to the containment atmosphere by aerosol generation has to be suppressed or at least be minimized. d) The generation of combustible gases has to be avoided or minimized.

In general such requirements cannot be achieved simultaneously and completely. Therefore compromises between costs of sophisticated retention devices covering all the above characteristics and safety improvements are aimed at.

From all the materials discussed and subjected to thermal and chemical interaction /178-181/, the following specimens seem to combine in particular the aspect of low costs and gain in retention capability:

- a) the different kinds of concrete as used for basemat construction  
i.e. lime stone, basaltic, magnetite concrete,
- b) refractory materials as magnesia ( $MgO$ ), alumina ( $Al_2O_3$ ), zirconia ( $ZrO_2$ ), graphite, fire brick, sodium borates,

c) materials of high melting points, Uranium oxide  $UO_2$ , Thorium oxide ( $ThO_2$ ).

Next, the particular interaction characteristics of some of the listed materials with a core melt or the coolant sodium are briefly described. A more systematic treatment of this topic has been given by Peckover /21/.

The decomposition of concrete under thermal attack of hot core debris or hot sodium is complex due to the great number of its constituents and different chemical compounds /182/. Powers et al. /182/ have demonstrated experimentally that the destruction of concrete by spallation and cracking due to thermal stresses is insignificant compared to the effect of thermal decomposition. In a simplified model, it is assumed that the thermal decomposition occurs at well defined temperature levels. The reaction zones are found within the heated concrete wall according to the position of the particular isotherms. The relevant reactions are endothermic except the formation of wollastonite ( $CaSiO_3$ ), which is exothermic. The characteristic reactions of the thermal decomposition are given in table 8 /151, 182/. The decomposition results essentially in a) the production of water vapor by evaporation of the free water content and by dehydration of chemically bound water (25-500 °C), b) the production of carbon dioxide ( $CO_2$ ) by decarboxilation of lime stone (500 - 1000 °C) and c) in generating a permeable layer of calcium oxide and siliceous compounds. The melting point of the latter compounds is in the range 1100 - 1400 °C and the enthalpy of melting is approximately 400 J/g /182/. The molten compounds are completely dissolved in the oxidic phase of the core melt. The gaseous products

Decomposition Temperature K	Decomposition Reaction	Heat of Decomposition kJ/mole
1573	$\text{SiO}_{2S} \rightarrow \text{SiO}_{2l}$	-8.53
	$\text{CaO} + \text{SiO}_2 \rightarrow \text{CaSiO}_3$	+88.5
	$\text{CaSiO}_{3S} \rightarrow \text{CaSiO}_{3l}$	-46.5
1167	$\text{CaCO}_3 \rightarrow \text{CaO} + \text{CO}_{2g}$	-165.5
796	$\text{Ca(OH)}_2 \rightarrow \text{CaO} + \text{H}_2\text{O}_g$	-99.5
400	$\text{H}_2\text{O}_f \rightarrow \text{H}_2\text{O}_g$	-39.4

Table 8 : Characteristics for the thermal decomposition of concrete /151, 182/.

water vapor and carbon dioxide which result as large volumes ( $5 \times 10^2 - 10^3$  times the volume of the decomposed concrete) percolate through the core melt and are partially reduced by the metallic phase to hydrogen and carbon monoxide. The erosion rate of concrete is predominantly determined by the heat flux from the melt to the surface of the concrete. For quasisteady state conditions a practically linear dependence between the two quantities is reported /184/. The penetration rate of metallic melts into concrete are generally higher than those of oxidic melts as has been demonstrated by experiments, see e.g. reference /186/. This means that the heat transfer from the pool bulk to the concrete surface is largely influenced by the Prandtl number of the molten pool. The thermal decomposition as well as the reduction and erosion processes are modelled in several codes, in particular in the LWR related codes for core melt concrete interaction, the codes CORCON /173a/ and WECHSL /151/.

Sodium-concrete reactions can be a major source term for energy, hydrogen and aerosols. The occurring chemical reactions may be subdivided in two groups: 1) The sodium reacts with the water vapor and the carbon dioxide, released from the concrete after thermal decomposition. 2) Sodium and its oxides react with the dehydrated calcareous and silicacious decomposition products of the concrete. The latter chemical reactions can be very complicated depending on the composition of aggregates in the particular concrete. A detailed experimental study of the chemistry of the sodium-concrete reaction can be found in reference /190/. In particular it was found

that the heat of reactions of aggregate materials varies in a wide range from  $200 \text{ Jg}^{-1}$  to  $2200 \text{ Jg}^{-1}$ . The prototypical reactions, contributing mostly to the heat generation, are listed in table 9.

Integral sodium-concrete reaction tests of intermediate scale (concrete surface area  $0.09 \text{ m}^2$ ) /191a, 191b/ and of large scale (horizontal concrete surface area  $0.66\text{-}1.45 \text{ m}^2$ ) /192/ have resulted in different gross behavior of the reacting components. In the intermediate scale tests, the interaction seems to be selflimiting since after some time a layer of inert reaction products separates the sodium pool from the concrete wall, or at least inhibits strongly penetration of chemically active compounds. In the large scale test, the tendency seems to be inverse. Here a relatively mild initial reaction is succeeded by vigorous chemical reaction which continues until all the sodium is consumed. No obvious explanation for this phenomenological discrepancy is currently available. Nevertheless efforts are being made to model the interaction process by computer codes /193, 194, 195/.

Magnesium oxide in the form of commercially available bricks (e.g. Harklase 98 %  $\text{MgO}$ ) is considered a favored sacrificial liner material for external core catchers. It has been demonstrated by out-of-pile experiments /180/ that  $\text{MgO}$  (melting point  $2800^\circ\text{C}$ ) and  $\text{UO}_2$  (melting point  $2850^\circ$ ) are miscible in the liquid state and form liquid solutions with an eutectic composition (50 mol %  $\text{MgO}$  in  $\text{UO}_2$ ). The range of the eutectic melting temperature was found from  $1800$  to  $2300^\circ\text{C}$ . Magnesia is dissolved smoothly into the molten  $\text{UO}_2$  in this temperature range. No cracking of the magnesia was

References	Chemical Reactions during Sodium Concrete Contact	Heat of Reaction kJ/mole H <sub>2</sub> O
	$2\text{Na} + \text{H}_2\text{O} \rightarrow \text{NaOH} + \left[ \text{NaH} \rightleftharpoons \text{Na} + \frac{1}{2} \text{H}_2 \right]$	+154
/195/	$4\text{Na} + \text{H}_2\text{O} \rightarrow \text{Na}_2\text{O} + \left[ 2\text{NaH} \rightleftharpoons 2\text{Na} + \text{H}_2 \right]$	+163
	$4\text{Na} + \text{CO}_2 \rightarrow 2\text{Na}_2\text{O} + \text{C}$	
	$\text{NaOH} + \frac{1}{2}\text{CaCO}_3 \rightarrow \frac{1}{2}\text{Na}_2\text{CO}_3 + \left[ \frac{1}{2}\text{Ca(OH)}_2 \rightarrow \frac{1}{2}\text{CaO} + \frac{1}{2}\text{H}_2 \right]$	+8,37
/193/	$2\text{NaOH} + \text{CaCO}_3 \rightarrow \text{Na}_2\text{CO}_3 + \text{H}_2\text{O} + \text{CaO}$	
	$4\text{Na} + 3\text{CaCO}_3 \rightarrow 2\text{Na}_2\text{CO}_3 + 3\text{CaO} + \text{C}$	+171
/195/	$4\text{Na} + 3\text{SiO}_2 \rightarrow 2\text{Na}_2\text{SiO}_3 + \text{Si}$	+133
/190/	$2\text{NaOH} + \text{SiO}_2 \rightarrow \text{Na}_2\text{SiO}_3$	
/190/	$\text{Na}_2\text{O} + \text{Na}_2\text{SiO}_3 \rightarrow \text{Na}_4\text{SiO}_4$	

Table 9: Typical reactions of sodium and sodium compounds during sodium concrete interaction.

observed, but  $UO_2$  diffused into the solid magnesia ahead of the melting front. Molten stainless steel poured into a magnesia crucible at temperatures of 1500 - 1600 °C produced no gas and, if any, very low erosion rates /178, 181/. Reported results concerning gas generation at higher temperatures, typically above 2500 °C, are controversy. Varela /113/ claims evidence of distinct gas generation in his furnace tests and in the SANDIA MP-5S /111/ whereas Stein et al. /180b/ found no evidence of that. Magnesia exposed to sodium at 850 °C showed no apparent interaction /196/ even if the silica content was near 4 %.

Alumina in pure form as  $Al_2O_3$  or as commercial refractory brick is also readily available. Pure alumina and  $UO_2$  form an eutectic reaction at about 1950 °C, but mixing between the eutectic and pure  $UO_2$  seems to be poor. However, alumina in the form of a silica containing refractory material appears to dissolve and distribute the  $UO_2$  throughout the melt /178, 185/. In medium scale tests the interaction of high alumina cement and stainless steel melt (208 kg) was investigated. During the 1000 sec test no erosion of the cement either by spallation nor by melting was observed. However, gases were generated during the interaction process at a moderate rate. The gas released from the top of the melt consisted mostly of hydrogen. This may be due to the thermal decomposition of the alumina cement which contained up to 2.3 % of water and the reduction of the water vapor by the metallic melt /178/. Alumina cement may be assessed as an attractive liner material if its water content can be further reduced. The reaction of alumina in contact with sodium at 850 °C depends on the amount of admixtures: 10 % silica gives some interaction, 10 % chromium oxide results in significant interaction /196/.

Graphite is being considered as a lower reactor shield in gas-cooled fast reactors, and besides has been proposed at a time as a cost-effective alternative liner for the core catcher of the German SNR-300. Testing the compatibility between  $UO_2$  and graphite at temperatures between  $1600\text{ }^{\circ}C$  and  $2400\text{ }^{\circ}C$ , Peehs et al. /187/ showed that  $UO_2$  is completely converted to Uranium carbide and gaseous carbon monoxide at  $2400\text{ }^{\circ}C$ . The conversion rates were high. In particular the reaction temperature was lowered to  $2000\text{ }^{\circ}C$  when a mixture of  $UO_2$  and stainless steel (SNR corium) was used in the test. Similar but more detailed and more comprehensive results were given by Fink et al. /188/. They conclude that the presence of material in which graphite is soluble could cause CO to be generated at an unacceptable rate. Therefore, due to this relatively high production rate of combustible CO gas, graphite falls back in the ranking list of cost effective sacrificial liner materials. Graphite has proved to be inert in contact with liquid sodium /196/.

Sodium borates e.g. Borax ( $Na_2O \times 2B_2O_3$ ) and sodium metaborate ( $Na_2O \times B_2O_3$ ) have been repeatedly proposed as sacrificial materials for the external core catcher of fast breeder reactors by M. Dalle Donne et al. /189 and literature in this reference/. Both materials dissolve  $UO_2$  and  $PuO_2$  and the oxidic fission products. As the main advantage the low melting point of these materials is put forward (borax  $740\text{ }^{\circ}C$ , metaborate  $966\text{ }^{\circ}C$ ). Indeed interaction tests of molten stainless steel and a sacrificial borax bed have shown that borax quenches rapidly high temperature melts. The quenched melts erode the borax slowly and nearly uniformly in horizontal and downward direction /182/. Besides for the Fast Breeder case the borine compound may serve as a neutron absorber and may exclude recriticalities

by dissolution of  $UO_2$  and  $PuO_2$ . With respect to the material properties (density, viscosity of the molten material, coefficient of thermal expansion) borax and sodium metaborate are well analysed /189/.

#### 4.9 Mechanical Integrity of Structures under High Thermal Loads

There is agreement among designers that in-vessel retention devices for core debris can be constructed even to cope with severest debris configurations i.e. molten debris pools /27, 197/. Such designs are likely to be very conservative since they have to be based on the elastic or at most elasto-plastic behavior of the structure materials and limit design rules have to be applied /198/. Moreover stress calculation and the calculations of the coolability of the particular structure must be carefully tuned.

The problem becomes more sophisticated, if the potential of thermo-mechanical loading of structures is to be assessed, which are not particularly designed for retention purposes and which themselves carry high structural loads. This type of analysis has been performed for the German Prototype SNR-300 for the PAHR phase following a core disruptive accident /199/. The calculation based on an elasto-plastic material behavior demonstrated that the internal loaded structures of the reactor tank possess a high capability for debris retention in the long term even under high thermal loads (i.e. hot spots of  $1200\text{ }^{\circ}\text{C}$  and temperature gradients in the steel structures of the order of  $100\text{ }^{\circ}\text{C/cm}$ ). Nevertheless, it is indicated that in the future for the analysis of structural loads at high temperatures more realistic material models should be

employed, which take into account the viscoelastic behavior of the structural material at high temperatures (which includes creep behavior) and multi-axial stress loads. Computational methods and constitutive equations for this have still to be developed and must be experimentally confirmed.

#### 4.10 Heat Transport from Hot Structures to Heat Sinks

Whether an accident can finally be terminated in vessel or not depends strongly on the availability of sufficient heat sinks and the availability of free flow paths from debris accumulations to heat sinks. The latter is to be demonstrated as part of the accident analysis and applies in particular for the heat removal from severely damaged core structures. As far as the integrity of internal structures of the reactor tank in particular the one of core catchers is concerned sufficient cooling has to be proved locally. For low flow velocities as they occur under conditions of natural circulation flow in a reactor tank a uniform distribution of the coolant flow may not be warranted due to thermal stratification and due to the specific positions of the heat sinks. This may result in dangerous hot spots and local failure of the in-vessel structures.

For in-vessel core catchers as presently under construction or design (see section 3), specific investigations on the local heat transfer have been carried out. These investigations are mainly concerned with the heat transfer from downward facing horizontal plates or inclined walls /200-202/. Good agreement was found between experimental and theoretical results for the special case of heat transfer from a horizontal downward facing plate by natural convection. This is demonstrated in figure 14.

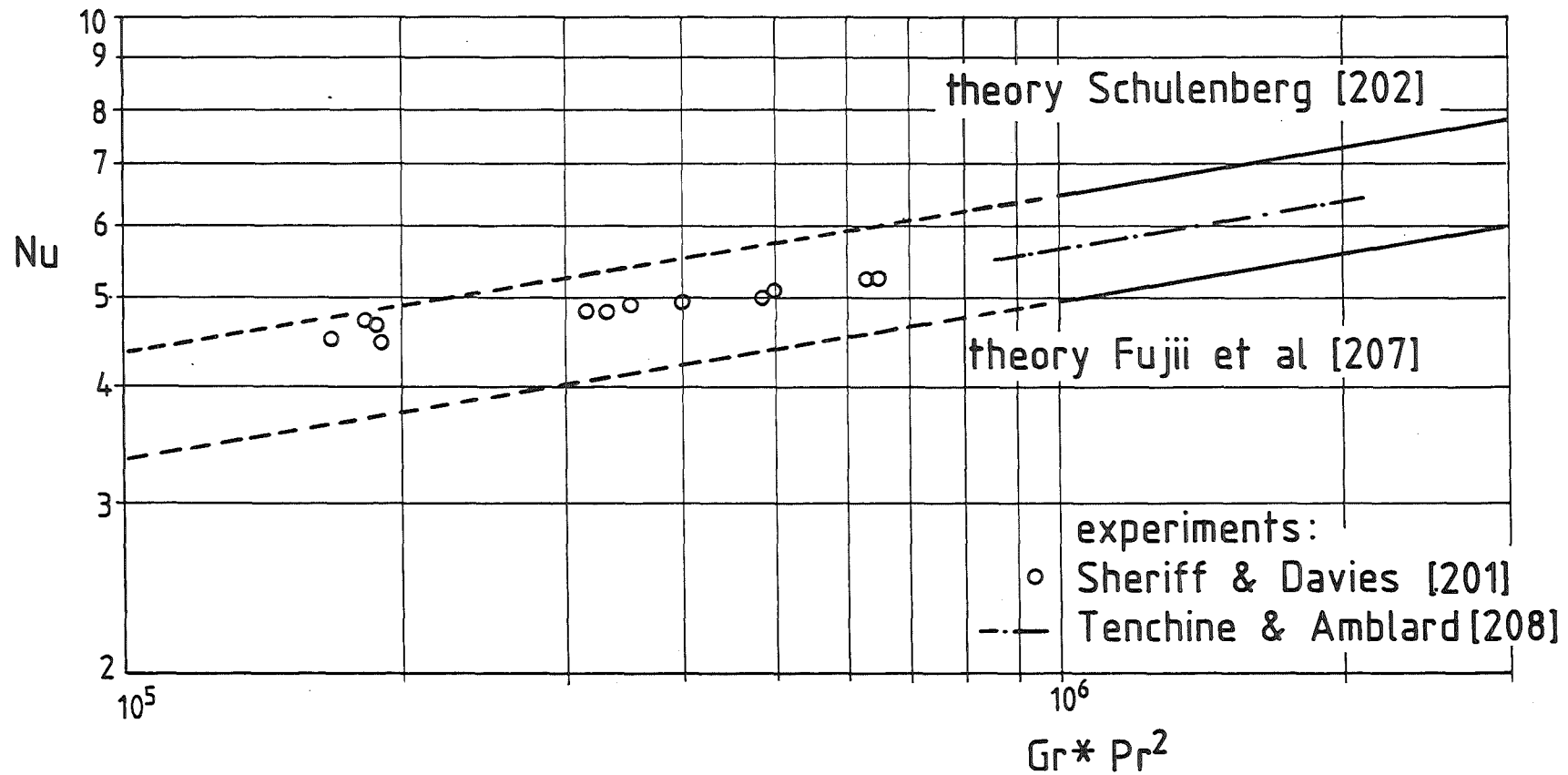


Fig. 14 Local Nusselt number for the heat transfer from a downward facing horizontal plate with uniform heat flux.

Up to date, the heat transport within the primary circuit and the reactor tank by mixed flow or by mere natural convection was mostly treated by lumped parameter single loop models. Equivalent codes are readily available /12, 203, 204/. These computer programs have been repeatedly tested by experimental data from out of pile mock up test facilities and from in pile low power and low flow tests.

Although these codes are useful to study the overall systems behavior i.g. average coolant temperatures under transient operation conditions they may fail completely if the temperatures of specific components in the tank are to be assessed or even predicted. These facts were put forward recently for pool type reactors by Webster /205/ who pointed out the difficulties in simulating certain features of the natural circulation tests at the British PFR. He proposed to use multi-loop models for simulating recirculating flows in subdomains of the reactor tank, in particular between the inner and outer pools and between the inner pool and the core. Such a procedure can improve the prediction of lumped parameter models for temperature and flow distributions in subdomains. Its further development and application deserves special attention and should be pursued rigorously in the future since this calculational method is faster than any two or even three-dimensional calculation for the flow and temperature field.

However, ultimately two- and three-dimensional models must be made available in order to analyze and study local flow phenomena in the reactor primary system, for instance, if due to accident conditions the primary reactor system is submitted to a skewed thermal hydraulic operation (e.g. loss of some of the provided heat sinks).

The COMMIX code presently under development at ANL /206/ is considered to serve as such an analytical tool for in vessel local flow behaviour. More specific experimental programs are needed, however, for the verification of this computer program in order to obtain reliable predictions even under the more complex accident conditions.

## 5. Summary and Conclusions

The investigations of Post Accident Debris Cooling can be considered as well advanced. Relevant problems concerning the integrity of safety barriers in the late phase of core melt down accidents have been identified. The key physical phenomena occurring when hot debris interacts with the reactor coolant and the structural material are understood. However, regarding the quantitative description of the interaction processes in specific reactor systems some uncertainties still exist. In order to further substantiate the present assessments of accident consequences and risks to the public from the extremely low probability core melt down event further research activities in the PAHR field should concentrate on the following items.

- The present analysis of the initial debris distribution, debris pile configuration and bed characteristics within the reactor vessel is to be substantiated. In particular the fragmentation efficiency of a jet of hot core melt released from the bottom of the fuel assemblies into the sodium pool of the lower plenum (LMFBR specific) should be quantified, since the debris retention

capability of the in-vessel structures can be initially destroyed by jet impingement or pressure loads due to energetic FCI.

- The safety margins of the post dryout behaviour of particle beds of core debris should be explored in more detail.
- The long term availability and proper location of heat sinks for active or passive decay heat removal from debris accumulations should be investigated. Moreover it must be shown that sufficiently free flow paths exist from the structures where debris can be deposited to the available heat sinks.
- The problem of creep fatigue and creep rupture and its relevance for long term integrity of structures under high thermal loads needs further evaluation.

Research progress in these areas will contribute to an improved assessment of the inherent debris retention capability of reactor structures and may promote much simpler designs of core catchers in the future, if such devices are required at all in future commercial reactors.

**Acknowledgement:**

The authors gratefully acknowledge critical comments from their colleagues Dr. L. Barleon, G. Hofmann, and Dr. M. Reimann.

Dr. L. Barleon has provided the table of thermophysical properties in the appendix.

Appendix:

Property	Symb.	Dimensions	UO <sub>2</sub>		References		Stainless Steel		References	
							1)	2)		
Density	$\rho$	10 <sup>3</sup> kg/m <sup>3</sup>	8.66		/A5/		6.93	5.82	/A5/	/A6/
Heat Conductivity	$\lambda$	W/mK	2.9	1.7	/A14/	/A7/	17.8	19.4	/A5/	/A2/
Specific Heat	$c_p$	10 <sup>3</sup> Ws/kgK	0.50		/A5/		0.78		/A5/	
Viscosity	$\mu$	10 <sup>-3</sup> kg/sm	4.3	5.7	/A5/	/A8/	6.42	8.89	/A5/	/A10/
Surface Tension	$\sigma$	N/m	0.45	0.522	/A5/	/A6/	1.50	1.57	/A5/	/A6/
Melting Point	$T_M$	K	3138		/A5/		1700		/A5/	
Boiling Point	$T_{BP}$	K	3520 <sup>3)</sup>		/A5/		3080		/A5/	
Heat of Fusion	$\Delta H_M$	10 <sup>6</sup> Ws/kg	0.283		/A5/		0.268		/A5/	
Heat of Vaporization	$\Delta H_V$	10 <sup>6</sup> Ws/kg	2.00 <sup>3)</sup>		/A5/		7.412		/A5/	
Volumetric Expansion	$\beta$	10 <sup>-4</sup> K <sup>-1</sup>	1.05		/A5/		0.903		/A5/	

Table 10 Thermophysical Properties of Core Melt Phases in the Liquid State

1) Stainless steel Nr. 304

2) Stainless steel Nr. 1.4970

3) Mixed oxide fuel UO<sub>2</sub>-PuO<sub>2</sub>

## Figure Captions

- Fig. 1 SNR-300 core-catcher.
- Fig. 2 The internal core-catcher in Super Phenix.
- Fig. 3 In-vessel core-catcher in CDFR.
- Fig. 4 In-vessel natural circulation flow in SNR-300 under PAHR conditions.
- Fig. 5 Particle-bed core retention device.
- Fig. 6 Particle size distribution obtained from fuel coolant interaction experiments.
- Fig. 7 Void fraction in a stratified particle bed.
- Fig. 8 Distribution of heat sources during a LWR-core-melt-down accident.
- Fig. 9 Overall Nusselt number versus internal Rayleigh number for single phase natural convection in saturated particle layers.
- Fig. 10 Dryout heat flux as a function of particle diameter.
- Fig. 11 Dryout heat flux versus bed height for in-pile and out-of-pile experiments with  $UO_2$ -particles and sodium as a coolant. Particle size: range 0.1-1 mm.
- Fig. 12 Schematic drawing of the MP-5S bed of the Sandia in-pile experiment /114/.
- Fig. 13 Evolution of a particle debris pile, schematically after Kayser and Le Rigoleur /115/.
- Fig. 14 Local Nusselt number for the heat transfer from a downward facing horizontal plate with uniform heat flux.

List of Tables

- Table 1 Release rates of fission products from a core melt in (%/min) for  $T = 2400^{\circ}\text{C}$  after Albrecht and Wild /69/.
- Table 2 Thermal conductivity relations for isotropic particle beds.
- Table 3.1 Group definitions of Table 3.2.
- Table 3.2 Single phase heat transfer correlations in debris beds.
- Table 3.3 Nomenclature of Table 3.2.
- Table 4.1 Group definitions and nomenclature of Section 4.53.
- Table 4.2 Dryout correlations for volumetrically heated top fed beds.
- Table 4.3 Channel length correlations.
- Table 5 Heat transfer from volume-heated pools;  
 $Nu_{\uparrow}$  - upward Nusselt number,  $Nu_{\rightarrow}$  - horizontal Nusselt number,  $Nu_{\downarrow}$  - downward Nusselt number.
- Table 6 Heat transfer from boiling and bubbling pools.
- Table 7.1 Heat transfer correlations corresponding to molten pool penetration into substrates.
- Table 7.2 Nomenclature of table 7.1
- Table 8 Characteristics for the thermal decomposition of concrete /151, 182/.
- Table 9 Typical reactions of sodium and sodium compounds during sodium concrete interaction.
- Table 10 Thermophysical properties of core melt phases in the liquid state.

## References

- /1/ Proceedings of Post-Accident Heat Removal (PAHR) Information Exchange; October 8-9, 1974;  
R.L. Coats Editor; SAND75-0497, NUREG 76-6505.
- /2/ The Second Annual Post-Accident Heat Removal (PAHR) Information Exchange, November 13-14, 1975.  
R.L. Coats Editor; SAND76-9008.
- /3/ Proceedings of the Third Post-Accident Heat Removal Information Exchange, November 2-4, 1977  
L. Baker, J.D. Bingle, Editors; ANL-78-10.
- /4/ Post-Accident Heat Removal - Proceedings of the Fourth Post Heat Removal (PAHR) Information Exchange Meeting, October 10-12, 1978; V. Coen, H. Holtbecker, Editors;  
European Applied Research Reports, Vol. 1, Number 6, 1978 (EUR 6595 EN).
- /5/ Post-Accident Debris Cooling - Proceedings of the Fifth Post Accident Heat Removal Information Exchange Meeting, 1982,  
U. Müller, C. Günther, Editors, G. Braun, Karlsruhe, ISBN3-7650-2034-6, 1983.
- /6/ M.S. Kazimi, J.C. Chen:  
A condensed review of the technology of POST ACCIDENT Heat Removal for the Liquid Metal Fast Breeder Reactor;  
Nuclear Technology, Vol. 38, 1978, pp. 339-366.

- /7/ Proceedings of the Fast Reactor Safety Meeting,  
April 1974, Beverly Hills, California, CONF-740401-P3.
- /8/ Proceedings of the International Meeting on Fast Reactor Safety  
and Related Physics, October 1976, Chicago, Illinois, CONF-761001.
- /9/ Proceedings of the International Meeting on Fast Reactor Safety  
Technology, August 1979, Seattle, Washington.
- /10/ Proceedings of the LMFBR Safety Topical Meeting,  
July 1982, Lyon, Ecully France.
- /11/ Thermal and Hydraulic Aspects of Nuclear Reactor Safety,  
Vol. 1+2, Ed. O.C. Jones, S.G. Bankoff, 1977.
- /12/ A.A. Agrawal, J.G. Guppy:  
Decay Heat Removal and Natural Convection in Fast Breeder  
Reactors;  
Hemisphere Publishing Corporation, 1982.
- /13/ Nuclear Reactor Safety Heat Transfer, Ed. O.C. Jones,  
Hemisphere Publishing Corporation, 1981.
- /14/ I.F. Jackson, M.G. Stevenson, J.F. Marchaterre, R.H. Sevy,  
R. Avery, K.O. Ott:  
Trends in LMFBR Hypothetical-Accident Analysis;  
in /7/, pp. 1241-1264.

- /15/ R. Fröhlich, W. Mascheck, P. Schmuck, R. Royl, D. Struwe:  
Analyse schwerer hypothetischer Störfälle; Vorgehen und  
Anwendung auf Reaktorentwürfe;  
KfK-Nachrichten 10, 3-4, S. 66-71, Kernforschungszentrum  
Karlsruhe.
- /16/ H. K. Fauske:  
Core Disruptive Accidents; in /13/, pp. 481-530.
- /17/ Deutsche Risikostudie Kernkraftwerke (1979)  
(Hrsg.: Gesellschaft für Reaktorsicherheit) Verlag TÜV  
Rheinland.
- /18/ B. Rivard:  
Review of In-Vessel Meltdown Modells; NUREG/CR-1493, 1980.
- /19/ E.L. Gluekler, L. Baker:  
Post-Accident Heat Removal in LMFBR's; in /11/, Vol. 2,  
pp. 285 - 319
- /20/ R.S. Peckover:  
The Use of Core Catchers in Fast Reactors; Proc. Fast  
Reactor Safety Conf., p. 833ff, Karlsruhe, October 1973.
- /21/ R.S. Peckover:  
Ex-Vessel Post-Accident Heat Removal; in /13/, pp. 603-646.
- /22/ J. Costa:  
In-Vessel Post-Accident Heat Removal; in /3/, pp. 581-601.

- /23/ H.J. Friedrich:  
SNR-300 Tank External Core Retention Device Design and  
Philosophy Behind it; in /2/, p. 333.
- /24/ H.J. Friedrich:  
Dynamic Behaviour of SNR-300 Core Retention Device in Ex-  
perimental Support of the Design Concept; in /3/, p. 303.
- /25/ H. Vossebrecker, H.J. Friedrich:  
In-Vessel Fuel Retention, Retrospective View of SNR-300 and  
Prospect of SNR-2; in /5/, pp. 225-333.
- /26/ C. Le Rigoleur, G. Kayser, G. Maurin, B. Magnon:  
The Thermal Core Catcher in Super Phenix I; in /10/, pp. 285-296.
- /27/ D. Broadley, R.S. Peckover, B.D. Turland, J.E. Palentine:  
The Evolution and Validation of Internal Core Debris Reten-  
tion in the UK LMFBR's; in /10/, p. III-257.
- /28/ H. Vossebrecker, G. Grönefeld, D. Becker:  
Kühlung und Rückhaltung des Brennstoffes im Reaktortank des  
SNR-300 nach Exkursionsstörfällen; INTAT 69.00119, August 1980.
- /29/ H. Vossebrecker, A. Kellner:  
Inherent Safety Characteristics of Loop Type LMFBR's; in /9/,  
Vol. II, pp. 554-566.

- /30/ E.L. Gluekler, A. Hundsbedt, S.T. Lam, A.F. Shadin:  
Analysis of In-Vessel Core Debris Retention in Large LMFBR's;  
in /10/, pp. III-409-417.
- /31/ M. Reimann, K. Hassmann:  
Analyse des Ablaufs hypothetischer Kernschmelzenunfälle;  
aus: Sammlung der Vorträge zum Jahreskolloquium 1980 des  
Projektes Nukleare Sicherheit, Karlsruhe, Nov. 1980,  
KfK 3070, 1981.
- /32/ T.E. Murley, R. DiSalvo, R. Sherry, M. Silberberg:  
NRC'S Core Melt Research Program and its Relation to Current  
Regulatory Acitivites; in /31/.
- /33/ J.P. Hosemann:  
Wechselwirkung mit der Containmentstruktur und Spaltprodukt-  
freisetzung beim Kernschmelzenunfall;  
Atomwirtschaft 27 (1982) 10.
- /34/ D.G. Swanson, I. Catton, V.K. Dhir:  
A Thoria Rubble Bed for Post Accident Core Retention;  
in /5/, pp. 307-312.
- /35/ J.D. Fish, M. Pilch, F.E. Arellano:  
Demonstration of Passively-Cooled Particle-Bed Core Retention;  
in /10/, pp. III-327-336.
- /36/ R.O. Wooton, H.I. Avci:  
MARCH, Code Description and User's Manual, NUREG/CR-1711, Oct. 1980.

- /37/ I. Catton:  
Some Considerations in Post-Accident Heat Removal; in /1/,  
pp. 11-56.
- /38/ J.E. Boudreau:  
Analytical Models and Related Experimental Needs for Post-  
Accident Heat Removal Research; in /2/, pp. 27-28.
- /39/ H. Mizuta:  
Fragmentation of Uranium Dioxide after Molten Uranium Dioxide-  
Sodium Interaction;  
J. Nucl. Science and Technology 11, pp. 480-487, Nov. 1974.
- /40/ E.S. Sowa, J.D. Gabor, J.R. Pavlik, J.C. Cassulo, C.J. Cook,  
L. Baker:  
Molten Core Debris-Sodium Interactions M-Series Experiments;  
in /9/, p. 733.
- /41/ T.Y. Chu, A.G. Beattie, W.D. Drotning, D.A. Powers:  
Medium-Scale Melt Sodium Fragmentation Experiments;  
in /9/, pp. 742-756.
- /42/ T.Y. Chu:  
Fragmentation of Molten Core Material by Sodium;  
in /10/, pp. III-487-498.
- /43/ M. Amblard, G. Berthoud:  
UO<sub>2</sub>-Na Interaction; The Corect II Experiments; Fourth CSNI  
Spec. Meeting on Fuel Coolant Interaction in Nuclear Reactor  
Safety, Bournemouth, UK, April 2-5, 1979, Vol.2, p.508 - 532  
CSNI Report Nr. 37.

- /44/ M. Amblard, H. Jacobs:  
Fuel-Coolant Interactions, The Corect II UO<sub>2</sub>-Na Experiment;  
in /9/, pp. 1512-1519.
- /45/ R.W. Wright, J.J. Barghusen, S.M. Zivi, M. Epstein, R.O. Ivins,  
R.W. Mouring:  
Summary of Autoclave TREAT Tests on Molten-Fuel-Coolant  
Interactions; in /7/, pp. 254-262.
- /46/ S.G. Bankoff:  
Vapor Explosion in Nuclear Reactor Safety Heat Transfer;  
in /13/, pp. 695-728.
- /47/ U. Schumann:  
Dampfexplosion - Physikalische Grundlagen und Bezug zur Reak-  
torsicherheit; Kernforschungszentrum Karlsruhe, KfK 3388,  
August 1982.
- /48/ M. Corradini, N.E. Todreas:  
Prediction of Minimum Particle Size Based on Thermal Stress  
Initiated Fracture Model;  
Nuclear Engineering and Design 53 (1979) pp. 105-116.
- /49/ R. Benz, L. Biasi, H. Schins:  
Debris Formation in Sodium; in /5/, pp. 22-27.
- /50/ T. Fujishior, T. Hoshi, S. Yanagihara, M. Ishikawa:  
A Study on Pressure Generation Caused by Fuel Failure in NSSR  
Experiments; Fourth CSNI Spec. Meet. on Fuel-Coolant Interac-  
tion in Nuclear Reactor Safety, Bournemouth, UK, April 2-5, 1979,  
CSNI-Report 37, Vol. 2, p. 588.

- /51/ R.R. Hobbins, B.A. Cook, R.E. Mason:  
LWR Debris from Severe In-Pile Transient Tests; in /5/,  
pp. 133-138.
- /52/ J.T. Larkins, M.A. Cunningham:  
Nuclear Plant Severe Accident Research Plan;  
NUREG-0900, Jan. 1983.
- /53/ A. Fiege:  
Severe Fuel Damage Investigations of KfK/PNS;  
Kernforschungszentrum Karlsruhe, KfK 3431B, 1983.
- /54/ D. Alvarez, M. Amblard:  
Fuel Leveling; in /5/, pp. 28-33.
- /55/ J.D. Gabor, J.C. Cassulo, D.R. Pedersen:  
The Effect of Particle Stratification on Debris Bed Dryout;  
in /5/, pp. 85-89.
- /56/ J.D. Gabor, L. Baker, J.C. Cassulo:  
Studies on Heat Removal and Bed Leveling of Induction-Heated  
Materials Simulating Fuel Debris; in /2/, pp. 89-100.
- /57/ J.B. Rivard, R.L. Coats:  
Post-Accident Heat Removal: An Overview of Some In-Vessel  
Safety Considerations; in /9/, Vol. II, pp. 709-720.
- /58/ L. Baker, D.R. Pedersen, E.S. Sowa, J.D. Gabor:  
Core Debris Accommodation Research, Statuts and Plans;  
in /10/, pp. III-389-398.

- /59/ S.S. Tsai:  
Core Debris Deposition in the Primary Heat Transport System  
Piping of LMFBR's; in /3/, pp. 92-98.
- /60/ W. Maschek, D. Struwe:  
Recriticality Considerations and Core Material Distribution  
in the Reactor Vessel of SNR-300 as Consequence of Unprotected  
LOSS OF FLOW Transients in the Mark IA-Core; in /9/, pp. 721-732.
- /61/ C. Le Rigoleur, G. Kayser, G. Maurin:  
The Internal Core Catcher in SUPER PHENIX I; in /10/, pp.  
III-285-295.
- /62/ T.R. England, R. Wilezynski, N.L. Whittemore:  
Cinder-7: An Interim Report for Users, LA-5885-MS, Los Alamos  
Scientific Laboratory (1975).
- /63/ D.R. Marr:  
An Users Manual for Computer Code RIBD-II, A Fission Product  
Inventory Code, HEDL-TME 75-26, Hanford Engineering Development  
Laboratory, 1975.
- /64/ M.J. Bell:  
ORIGEN - The ORNL Isotope Generation and Depletion Code;  
ORNL-4628 Oak Ridge National Laboratory (1973).
- /65/ B.D. Turland, R.S. Peckover:  
The Distribution of Fission Product Decay Heat;  
in /3/, pp. 17-25.

- /66/ Mme. M. Berlin, E. de Montaingnac, J. Dufresne, G. Geisse:  
Evaluation of the Sodium Retention Factors for Fission Products  
and Fuel; in /11/, p. III-369-380.
- /67/ J. Fisher, J.D. Schilb, M.G. Chasanov:  
Investigation of the Distribution of Fission Products Among  
Molten Fuel and Reactor Phases; Journal of Nuclear Materials  
48(1973) 233-240.
- /68/ P. Parmentier, D. Damien:  
Residual Power Distribution Between the Phases of a Molten  
Pool From Out-of-Pile Experiments; in /11, p. III-543-546.
- /69/ H. Albrecht, H. Wild:  
Investigation of Fission Product Release by Annealing and Melting  
of LWR Fuel Pins in Air and Steam; Proceedings of the Topical  
Meeting on Reactor Safety Aspects of Fuel Behaviour,  
August 1981, Sun Valley.
- /70/ M. Reimann:  
Private communication, 1981.
- /71/ H. Kämpf, G. Karsten:  
Effects of Different Types of Void Volumes on the Radial  
Temperature Distribution of Fuel Pins; Nuclear Applica-  
tions & Technology, Vol.9, pp. 288-300, Sept. 1970.

- /72a/ B. Schulz:  
On the Thermal Conductivity and Viscosity of Debris Beds;  
NUREG/CP 0014, Vol. 3, pp. 1967-1978.
- /72b/ B. Schulz:  
Die Abhängigkeit der Feldeigenschaften zweiphasiger Werkstoffe  
von ihrem Gefügebau; Theoretische Überlegungen und experi-  
mentelle Prüfung am Beispiel der Wärmeleitfähigkeit von Cermets.  
KfK-Bericht 1988, 1974, Kernforschungszentrum Karlsruhe.
- /73/ I. Cook, R.S. Peckover:  
Effective Thermal Conductivity of Debris Beds;  
in /5/, pp. 40-45.
- /74/ H.W. Godbee, W.T. Ziegler:  
Thermal Conductivities of MgO, Al<sub>2</sub>O<sub>3</sub>, and ZrO<sub>2</sub> Powders to 850 °C,  
II Theoretical; J. Appl. Phys. Vol. 37, pp. 56-65 (1966).
- /75/ P. Zehner, E.U. Schlünder:  
Wärmeleitfähigkeit von Schüttungen bei mäßigen Temperaturen;  
Chemie Ingenieur Technik 42, 1970, pp. 933-941.
- /76/ E. Achenbach:  
Pressure drop, forced convective, free convective and radiant  
heat transfer in pebble beds; in /5/, pp. 204-213.
- /77/ J.E. Gronager, M.L. Schwarz, R.J. Lipinski:  
PAHR Debris Bed Experiment D-4; NUREC/CR-1809, SAND 80-2146, R-7.

- /78/ G.W. Mitchell, R.J. Lipinski, M.L. Schwarz:  
Heat Removal From a Stratified  $UO_2$ -Sodium Particle Bed;  
NUREG/CR-2412, SAND 81-1622, R-7, 1982.
- /79/ G.W. Mitchell, C.A. Ottinger:  
The D7 Experiment: Heat Removal from a Shallow Stratified  
 $UO_2$ -Sodium Particle Bed; in /5/, pp. 90-95.
- /80/ R.D. Gasser, M.S. Kazimi:  
Onset of Convection in a Porous Medium With Internal Heat  
Generation;  
Journal of Heat Transfer, Febr. 1976, pp. 49-54.
- /81/ B.D. Turland:  
Convection in Debris Beds?  
in /5/, pp. 96-101.
- /82/ W.J. Sun:  
Convective Instability in Superposed Porous and Free Layers;  
University of Minnesota, Ph.D., 1973, Engineering,  
Aeronautical.
- /83/ R.J. Buretta, A.S. Berman:  
Convective Heat Transfer in a Liquid Saturated Porous Layer;  
Journal of Applied Mechanics, June 1976, pp. 249-253.

- /84/ H.C. Hardee, R.H. Nilson:  
Natural Convection in Porous Media with Heat Generation;  
Nuclear Science and Engineering 63, 119-132 (1977).
- /85/ F.A. Kulacki, R.G. Freeman:  
A Note on Thermal Convection in a Saturated Heat-Generating  
Porous Layer;  
Journal of Heat Transfer, Febr. 1979, Vol. 101, 169-171.
- /86/ S.J. Ree, V.K. Dhir, I. Catton:  
Natural Convection Heat Transfer in Beds of Inductively Heated  
Particles;  
Journal of Heat Transfer, Vol. 100, Febr. 1978, 78-85.
- /87/ L. Barleon, H. Werle:  
Debris Bed Investigation With Adiabatic and Cooled Bottom;  
Proc. of the 9th Meet. of the Liquid Metal Boiling Working  
Group, Rome, 1980.
- /88/ T. Schulenberg, U. Müller:  
Natural Convection in Saturated Porous Layers with Internal  
Heat Sources; International Journal of Heat and Mass Transfer,  
Accepted for publication (1983).
- /89/ J.B. Rivard:  
Post Accident Heat Removal: Debris Bed Experiments D-2 and D-3;  
NUREG/CR-0421, SAND 78-1238 R-7.

- /90a/ J.M. Buchlin, C. Benocci, C. Joly, A. Siebertz:  
A Two-Dimensional Finite Difference Modeling of the Thermo-  
hydraulic Behavior of the PAHR Debris up to Extended Dryout;  
in /5/, pp. 265-271.
- /90b/ J.-M. Buchlin, C. Benocci:  
Theoretical Models of PAHR Phenomenology - State of the Art -;  
10th Liquid Metal Boiling Working Group Meeting, Karlsruhe,  
Kernforschungszentrum, October 27-28, 1982.
- /91/ L. Baker, R.E. Faw, F.A. Kulacki:  
Post-Accident Heat Removal - Part I: Heat Transfer within an  
Internally Heated, Nonboiling Liquid Layer.  
Nuclear Science and Engineering 61, 222-230, 1976.
- /92/ D. Squarer, A.T. Pieczynski, L.E. Hochreiter:  
Effect of Debris Bed Pressure, Particle Size, and Distribution  
on Degraded Nuclear Reactor Core Coolability.  
Nuclear Science and Engineering 80, 2-13 (1982).
- /93/ R.J. Lipinski:  
A Model for Boiling and Dryout in Particle Beds.  
NUREG/CR-2646, SAND 82-0765.
- /94/ V.K. Dhir, I. Catton:  
Dryout Heat Fluxes for Inductivity Heated Particulate Beds;  
J. Heat Transfer 99, 250-256 (1977).
- /95/ S.W. Jones, M. Epstein, J.D. Gabor, J.C. Cassulo, S.G. Bankoff:  
Investigation of Limiting Boiling Heat Fluxes from Debris Beds;  
Trans. ANS, 35, 361-363 (1980).

- /96a/ E.S. Sowa, I.C. Hesson, R.H. Gebner, G.T. Goldfuss:  
Heat Transfer Experiments through Beds of  $UO_2$  in Boiling Sodium;  
Trans. Am. Nucl. Soc., 14, 2, 725 (1971).
- /96b/ E.S. Sowa, D.R. Pedersen, J. Pavlik, R. Purviance:  
Experiments and Procedure for Bottom Heating Heat Transfer  
Experiments Through  $UO_2$  Debris Beds in Sodium;  
in /5/, pp. 114-118.
- /97/ R.R. Ostensen, R.J. Lipinski:  
A Particle Bed Dryout Model Based on Flooding;  
Nucl. Science and Eng. 79, 110-113 (1981).
- /98a/ G.L. Shires, G.F. Stevens:  
Dryout During Boiling in Heated Particle Beds;  
AEEW-M1779, UKAEA, Winfrith, England (1980).
- /98b/ G.F. Stevens, R. Trenberth:  
Experimental Studies of Boiling Heat Transfer and Dryout  
in Heat Generating Particulate Beds in Water at 1 Bar;  
in /5/, pp. 108-113.
- /99/ S.W. Jones, L. Baker, S.G. Bankoff, M. Epstein, D.R. Pedersen:  
A Theory for Prediction of Channel Depth in Boiling Particulate  
Beds; J. Heat Transf. 104, 806-808 (1982).
- /100/ L. Barleon, K. Thomauske, H. Werle:  
Bottom Cooling of Particulate Debris Beds;  
in /5/, pp. 119-125.

- /101/ G. Hofmann:  
On the Location and Mechanism of Dryout in Top-Fed and Bottom-Fed Particulate Beds; in /5/, pp. 186-191.
- /102a/ A.S. Naik, V.K. Dhir:  
Forced Flow Evaporative Cooling of a Volumetrically Heated Porous Layer; Int. J. Heat Mass Transfer 25, 541-552 (1982).
- /102b/ D.H. Cho, D.R. Armstrong, L. Bova, S.H. Chan, G.R. Thomas:  
Experiments on Quenching of a Hot Debris Bed;  
in /5/, pp. 145-150.
- /103/ T. Ginsberg, J. Klein, J. Klages, C.E. Schwarz, J.C. Chen:  
Phenomenology of Transient Debris Heat Removal;  
in /5/, pp. 151-158.
- /104/ L. Barleon, H. Werle, R.J. Lipinski:  
Heat Transfer in Particulate Debris Beds; in /10/, pp. III-337-346.
- /105/ L. Barleon, K. Thomauske, H. Werle:  
Dependence of Dryout Heat Flux on Particle Diameter and Bed Height and Effects of Stratification and Bed Reconfiguration;  
in /5/, pp. 74-78.
- /106/ J.C. Gabor, J.C. Cassulo, D.R. Pedersen:  
The Effect of Particle Stratification on Debris Bed Dryout;  
in /5/, pp. 85-89.

- /107/ R.J. Lipinski, J.E. Gronager, M. Schwarz:  
Particle Bed Heat Removal with Subcooled Sodium: D-4 Results  
and Analysis; Nucl. Techn. 58, 369-378 (1982).
- /108/ D. Schwalm, R. Nijsing:  
The Influence of Subcooling on Dryout Inception in Sodium-  
Saturated Fuel Particle Beds with Top Cooling and Adiabatic  
Bottom; Nucl. Eng. Design 70, 201-208 (1982).
- /109/ A.W. Reed:  
The Effect of Channeling on the Dryout of Heated Particulate  
Beds Immersed in a Liquid Pool;  
Ph.D. Thesis, Mass. Inst. of Techn., Cambridge, MA (1982).
- /110/ J.D. Gabor, E.S. Sowa, L. Baker, jr., J.C. Cassulo:  
Studies and Experiments on Heat Removal from Fuel Debris in  
Sodium; Proc. of ANS FAST REACTOR Safety Meeting, Beverly  
Hills, CA, April 1974. pp. 823-844.
- /111/ J.T. Hitchcock, J.E. Kelly:  
Post-Test Examination of the In-Pile Molten Pool Experiments.  
Trans. Am. Nucl. Soc. 43, 515-516, 1982.
- /112/ D.W. Varela:  
Molten Steel Behaviour in PAHR Debris Beds.  
Trans. Am. Nucl. Soc. 38, 388-389, 1981.
- /113/ D.W. Varela:  
High-Temperature Magnesium Oxide Interactions with  $UO_2$ ;  
Trans. Am. Nucl. Soc. 34, 546, 1980.

- /114/ H.G. Plein, R.J. Lipinski, G.A. Carlson, D.W. Varela:  
Summary of the First Three In-Core PAHR Molten Fuel Pool Experiments; in /9/, Vol. I, p. 356.
- /115/ G. Kayser, C. Le Rigoleur:  
The Main Problems of an Internal Core-Catcher for a Pool Type Commercial LMFBR; in /4/, pp. 380-387.
- /116/ H. Backs, H. Holtbecker, C. Joly, M. Soenen, D. Rousseau, J. Vayrat:  
The European PAHR-In-Pile-Programme, Objectives and General Layout; in /10/, pp. III-317-326.
- /117/ P. Hofmann, H. Holleck, C. Politis, A. Skokan:  
Konstitution und Reaktionsverhalten von LWR-Komponenten beim Coreschmelzen; KfK 2242, Kernforschungszentrum Karlsruhe.
- /118/ D.G. Swanson, E.H. Zehms, D.M. Goddard, C.Y. Ang, H.L. van Passen, G.D. Kidwell, A.R. Marchese:  
Interactions Between Molten Core Debris and Core Containment Materials; Trans. Am. Nucl. Soc. Vol. 27, 1977, p. 659.
- /119/ R.S. Peckover, I.H. Hutchinson:  
Convective Rolls Driven by Internal Heat Sources.  
Physics of Fluids 17, 1369-1371, 1974.
- /120a/ Mayinger, F., Jahn, M., Reineke, H.H., Steinberner, U.:  
Untersuchungen thermohydraulischer Vorgänge sowie Wärmeaustausch in der Kernschmelze. Abschlußbericht BMFT-RS 48./1.

- /120b/ F. Mayinger, H.H. Reinecke, R. Schramm, U. Steinbrenner:  
Verhalten der Kernschmelze beim Hypothetischen Störfall,  
Kennwort: Thermohydraulik der Schmelze, BMFT RS 166.
- /121/ M. Jahn, H.H. Reinecke:  
Free Convective Heat Transfer with Internal Heat Sources,  
Calculations and Measurements. Proc. 5th, International Heat  
Transfer Conf., Tokyo, Sept. 1974, Vol. III, NC2.8, p. 74-78.
- /122/ H.H. Reinecke, R. Schramm, U. Steinbrenner:  
Heat Transfer from a Stratified Two Fluid System with  
Internal Heat Sources; in /4/, pp. 87-97.
- /123a/ I. Catton, A.J. Suo-Antilla:  
Heat Transfer from a Volumetrically Heated Horizontal Fluid  
Layer; Proc. 5th Int. Heat Transfer Conf., Tokyo, Sept. 1974,  
Vol. III, Paper NC2.7, pp. 69-73.
- /123b/ A.J. Suo-Antilla, I. Catton:  
The Effect of a Stabilizing Temperature gradient on Heat  
Transfer from a Molten Fuel Layer with Volumetric Heating;  
J. Heat Transfer 97, 544-548, 1975.
- /124/ N.K. Lambha, S.A. Korpela, F.A. Kulacki:  
Thermal Convection in a Cylindrical Cavity with Uniform Volu-  
metric Energy Generation. Paper NC-22, Proc. 6th Int. Heat  
Transfer Conf. Toronto, 1978.

/125/ G. Grötzbach:

Spacial Resolution Requirements for Numerical Simulation of Internally Heated Fluid Layers. Numerical Methods in Laminar and Turbulent Flow. Proc. Second International Conf. Venice, July 1981. Ed. C. Taylor, B.A. Schrefler, pp. 593-604.

/126/ F.A. Kulacki, A.A. Emara:

Steady and transient thermal convection in a fluid layer with uniform volumetric energy sources;  
J. Fluid Mech. (1977), Vol. 83, 375-395, 1977.

/127/ F.A. Kulacki, M.E. Nagele:

Natural Convection in a Horizontal Fluid Layer with Volumetric Energy Sources; J. of Heat Transfer, pp. 204-211, 1975.

/128/ A.J. Suo-Antilla, I. Catton:

An Experimental Study of a Horizontal Layer of Fluid with Volumetric Heating and Unequal Surface Temperature;  
AIChE Symposium Series No. 164, Vol. 73, Nat. Heat Transf. Conf., St. Louis, pp. 72-77, 1976.

/129/ J.C. Ralph, R. Mc Greevy, R.S. Peckover:

Experiments in Turbulent Thermal Convection Driven by Internal Heat Sources; in: Heat Transfer and Turbulent Bouyant Convection, Eds. D.B. Spalding, N. Afgan, Vol. II, pp. 587-599, Hemisphere 1977.

/130/ P. Boon-Long, T.W. Lester, R.E. Faw:

Convective Heat Transfer in an Internally Heated Horizontal Fluid Layer with Unequal Boundary Temperatures;  
Int. J. Heat Mass Transfer, Vol. 22, 437-445, 1979.

/131a/ G. Fieg, H. Werle:

Experimental Investigation of Heat Transfer in Pools;  
in /9/, Vol. I, pp. 346-355.

/131b/ F.B. Cheung:

Correlation Equation for Turbulent Thermal Convection in a  
Horizontal Fluid Layer Heated Internally and from Below;  
J. Heat Transfer, Vol. 100, 416-422, 1978.

/132a/ F.B. Cheung:

Natural Convection in a Volumetrically Heated Fluid Layer at  
High Rayleigh Numbers;  
Int. J. Heat Mass Transfer, Vol. 20, pp. 499-506, 1977.

/132b/ R.F. Bergeholz, M.M. Chen, F.B. Cheung:

Generalization of Heat-Transfer Results for Turbulent Free  
Convection Adjacent to Horizontal Surfaces;  
Int. J. Heat Mass Transfer, Vol. 22, pp. 763-769, 1979.

/133a/ G. Fieg:

Heat Transfer Measurements of Internally Heated Liquids in  
Cylindrical Convection Cells; in /4/, pp. 144-153.

/133b/ J.D. Gabor, L. Baker, J.C. Cassulo, D.J. Erskine, J.G. Warner:

Heat Transfer to Curved Surfaces from Heat Generating Pools.  
J. Heat Transfer, 1980, Vol. 102, pp. 519-524.

/134/ J.D. Gabor, J.C. Cassulo, P.C. Ellison:

Heat Transfer from Internally Heated Hemispherical Pools.  
ASME Heat Transfer Division; ASME/AICHE National Heat Transfer  
Conference, Orlando, July 1980, paper 80-HT-16.

- /135/ R.P. Stein, L. Baker, W.H. Gunther, C. Cook:  
Heat Transfer from Internally-Heated Molten  $UO_2$  Pools.  
in /4/, pp. 154-163.
- /136/ R.P. Stein, R. Farhadieh, D.R. Pedersen, W.H. Gunther, R.T.  
Purviance:  
Experimental Investigations of Long-Term Interactions of Molten  
 $UO_2$  with  $MgO$  and Concrete at Argonne National Laboratory;  
in /10/, pp. III-587-596.
- /137/ L. Baker, jr., M.G. Chasanov, J.D. Gabor, W.H. Gunther,  
J.C. Cassulo, J.D. Bingle, G.A. Mansoori:  
Heat Removal from Fuel Pools; in /8/, pp. 2056-2071.
- /138/ Cho, D.H. Chan, S.H., Hauser, G.M.:  
Radiative Heat Transfer in a Horizontal Molten Fuel Layer  
with Volumetric Heating;  
Trans. Am. Nucl. Soc. Vol. 30, pp. 473-474, 1978.
- /139/ M. Epstein, F.B. Cheung, T.C. Chawla, G.M. Hauser:  
Effective Thermal Conductivity for Combined Convection -  
Radiation Heat Transfer in a Molten Oxide Fuel Layer;  
Trans. Am. Nucl. Soc. Vol. 35, pp. 363-364, 1980.
- /140/ T.C. Chawla, S.H. Chan, F.B. Cheung, D.H. Cho:  
Combined Natural Convection and Radiation in a Volumetri-  
cally Heated Fluid Layer;  
J. Heat Transfer, Febr. 1980, Vol. 102, 81-85.

- /141/ E.E. Anderson:  
Radiative Heat Transfer in Molten  $UO_2$  Based on the Rosseland Diffusion Method; Nuclear Technology, Vol. 30, 1976, pp. 65-70.
- /142/ T.C. Chawla, S.H. Chan, F.B. Cheung:  
The Effect of Radiation Heat Transfer on Maximum Nonboiling Thickness of a Molten Oxide Fuel Layer with Decay Heating. Trans. Am. Nucl. Soc. Vol. 33, pp. 521-522, 1979.
- /143/ M. Bober, J. Singer, R. Wagner:  
On the radiative heat transfer in Liquid Urania;  
in /5/, pp. 59-64.
- /144/ J.D. Gabor, L. Baker, J.C. Cassulo, G.A. Mansoori:  
Heat Transfer from Heat-Generating Boiling Pools.  
Nuclear, solar, and process heat transfer, AIChE Symposium Series 164, Vol. 73, 1977, pp. 78-85.
- /145/ W.R. Gustavson, M.S. Kazimi, J.C. Chen:  
Heat Transfer and Fluid Dynamics in a Volume-heated Boiling Pool; in /8/, Vol. IV, pp. 2066-2076.
- /146/ G.A. Green, O.C. Jones, C.E. Schwarz, N. Abuaf:  
Heat Removal Characteristics of Volume Heated Boiling Pools with Inclined Boundaries.  
NUREG/CR-1357, BNL-NUREG 51 157, April 1980.
- /147/ T.C. Chawla, S.H. Chan:  
Heat Transfer from Heat-Generating Boiling Pools Pertaining to Transition Phase and PAHR.  
Trans. Am. Nucl. Soc. Vol. 39, 1981, pp. 666-667.

- /147a/ T.C. Chawla, S.H. Chan:  
Heat Transfer from Vertical/Inclined Boundaries of Heat-  
Generating Boiling Pools; J. Heat Transf. Vol.104, 465-473,1982.
- /148/ D.H.Cho, G.A. Lambert, S.W. Jones:  
Closed-Pool Boil-up Experiment.  
Trans. Am. Nucl. Soc. Vol. 43, 1982, pp. 510-511.
- /149/ T. Ginsberg, O.C. Jones, C.E. Schwarz, J.C. Chen:  
Observations of Flow Characteristics of Volume-Heated  
Boiling Pools; BNL-NUREG 24270, BNL (1977).
- /150/ H. Alsmeyer, M. Reimann:  
On the Heat and Mass Transport Processes of a Horizontal  
Melting or Decomposing Layer under a Molten Pool; in:  
Nuclear Reactor Safety Heat Transfer, The Winter Annual  
Meeting of the American Society of Mechanical Engineers,  
Atlanta, Georgia, Nov. 27-Dec. 2, 1977, edited by A.A.  
Bishop, F.A. Kulacki, S.G. Bankoff, O.C. Jones, jr.,  
pp. 47-62.
- /151/ M. Reimann, W.B. Murfin:  
The Wechsel Code: A Computer Program for the Interaction of a  
Core Melt with Concrete; Model Description and User's Manual;  
KfK 2890, Kernforschungszentrum Karlsruhe, 1981.
- /152/ H. Alsmeyer, M. Peehs, D. Perinic:  
Untersuchung der Wechselwirkung einer Kernschmelze mit Beton  
in der BETA Versuchsanlage; in: Sammlung der Vorträge zum  
Jahreskolloquium 1982 des Projektes Nukleare Sicherheit, Kern-  
forschungszentrum Karlsruhe, Okt. 1982, KfK 3470, 1983.
- /153/ H. Werle:  
Enhancement of Heat Transfer Between Two Horizontal Liquid  
Layers by Gas Injection at the Bottom. KfK 3223, Kernfor-  
schungszentrum Karlsruhe (1981).

- /154/ H. Werle:  
Experimental Investigation of Heat Transfer Between Two  
Horizontal Liquid Layers with Gas Injection.  
in /4/, pp. 164-171.
- /155/ G.A. Greene, C.A. Schwarz:  
Interfacial Heat Transfer Between Overlying Liquid Layers  
with Gas Agitation.  
Trans. Am. Nucl. Soc. 39, pp. 1050-1051, Nov. 1981.
- /156/ G.A. Greene, C.A. Schwarz:  
An Approximate Model for Calculating Overall Heat Transfer  
Between Overlying Immiscible Liquid Layers with Bubble-Induced  
Liquid Entrainment; in /5/, pp. 251-257.
- /157/ R.D. Haberstroh, R.D. Reinders:  
Conduction-Sheet Model for Natural Convection Through a Density-  
Stratified Interface Int. J. Heat Mass Transfer, Vol. 17,  
pp. 307-311, 1974.
- /158/ R.E. Faw, L. Baker:  
Post-Accident Heat Removal - Part II: Heat Transfer from an  
Internally Heated Liquid to a Melting Solid;  
Nuclear Science and Engineering 61, 231-338 (1976).
- /159/ G. Fieg, H. Werle:  
Heat Transfer Measurements from Internally Heated Liquids  
Enclosed by Non-Melting and Melting Boundaries; in /3/,  
pp. 153-160.

- /160/ D.K. Felde, Z. Musicki, S.I. Abdel-Khalik:  
Growth of Volumetrically-Heated Pools in Miscible Gas-Releasing  
Solid Beds; in /4/, pp. 253-262.
- /161/ H. Alsmeyer  
IRB, Kernforschungszentrum Karlsruhe, private communication.
- /162/ B.D. Turland, R.S. Peckover, T.A. Dullforce:  
On the Stability of Advancing Melting Fronts to Spacial  
Perturbations; in /3/, pp. 172-178.
- /163/ B.D. Turland, R.S. Peckover:  
The stability of planar melting fronts in two-phase thermal  
Stefan problems;  
J. Inst. Maths Applics 1980, 25, 1-15.
- /164/ R. Farhadieh, L. Baker  
Heat Transfer Phenomenology of a Hydrodynamically Unstable  
Melting System; J. Heat Transfer, Vol. 100, 1978, 305-310.
- /165/ R. Farhadieh  
Downward Heat Transfer in a Miscible Melting System  
Trans. Am. Nucl. Soc. 38, 1981, pp. 389-390.
- /166/ G. Eck:  
Untersuchungen zur vertikalen Ausbreitung einer beheizten  
Schmelze in einem festen löslichen Bett;  
Kernforschungszentrum Karlsruhe, KfK 3267, 1982.

- /167/ M.M. Chen, L. Baker:  
The Heat Transfer Mechanism Associated with Immersed Melting Surfaces; Trans. Am. Nucl. Soc. Vol. 28, 1978, 457-458.
- /168/ R. Farhadieh, M.M. Chen:  
Mechanism Controlling the Downward and Sideward Penetration of a Hot Liquid Pool into a Solid; in /3/, pp. 187-191.
- /169/ K. Taghavi-Tafreshi, V.K. Dhir, I. Catton:  
Thermal and Hydrodynamic Phenomena Associated with Melting of a Horizontal Substrate Placed Beneath a Heavier Immiscible Liquid; J. Heat Transfer, Vol. 101, 1979, 318-325.
- /170a/ R. Farhadieh, M. Epstein, J.D. Bingle:  
Downward Penetration of a Hot Liquid Pool into Underlying Meltable Solid; Trans. Am. Nucl. Soc. Vol. 35, 1980, 363-364.
- /170b/ R.F. Bergholz, R. Bjorge:  
Bubble-Induced Heat Transfer in a Heat Generating Liquid Layer; in /3/, pp. 361-368.
- /171/ R. Schramm:  
Berechnung von Konvektionsformen bei unmischbaren Fluiden mit inneren Wärmequellen; Dissertation Fakultät für Maschinenwesen, Universität Hannover, 1979.
- /172/ J. Beyer, H. Alsmeyer:  
IRB, Kernforschungszentrum Karlsruhe, Private Communication.

/173a/ R. Farhadieh:

Downward Penetration of a Hot Liquid Pool into a Gas Releasing Miscible Solid Surface; Nuclear Science and Engineering 78, 294-304, 1981.

/173b/J J.M. Muir, R.R. Cole, M.L. Corradini, M.A. Ellis:

CORCON-MODI: An Improved Model for Molten-Core/Concrete Interaction; NUREG/CR-2141-SAND 80-2415 R3.

/174/ V.K. Dhir, J.N. Castle, I. Catton:

Role of Taylor Instability on Sublimation of a Horizontal Slab of Dry Ice; J. Heat Transfer Vol. 99, 411-418 (1977).

/175/ M. Reimann, H. Alsmeyer:

Hydrodynamic and Heat Transfer Processes of Dry Ice Slabs Sublimating in Liquid Pools; Proc. 7th Int. Heat Transf. Conf. München 1982, Vol. 4, PB26, pp. 164-172.

/176/ H.H. Reinecke, L.Rinkleff, R. Schramm:

Heat Transfer Between Molten Core Material and Concrete; in /3/, pp. 114-121.

/177/ R. Schramm:

Untersuchungen zur Wechselwirkung von Kernschmelzen und Beton; BMFT-FB (RS 166-79-05) Abschlußbericht Bd. Ib, TU Hannover, Sept. 1980.

/178/ D.A. Powers:

A Survey of Melt Interactions with Core Retention Material; in /9/, pp. 379-388.

- /179/ J.K. Fink, J.J. Heiberger, L. Leibowitz:  
Interaction of  $UO_2$  with Reactor Materials; in /3/, pp. 415-423.
- /180a/ R.P. Stein, L. Baker, W.H. Gunther, C. Cook:  
Interaction of Heat Generating Molten  $UO_2$  with Structural  
Materials; in /3/, pp. 398-407.
- /180b/ R.P. Stein, R. Farhadieh, D.R. Pedersen, W.H. Gunther, R.T.  
Purviance:  
Experimental Investigation of Long-Term Interactions of  
Molten  $UO_2$  with  $MgO$  and Concrete at Argonne National Labora-  
tories; in /10/, pp. III-587-596.
- /181/ D.G. Swanson, E.H. Zehms, C.-Y. Ang, H.L.L. van Paassen:  
Molten Core Debris Interaction with Core Containment Materials;  
in /3/, pp. 408-414.
- /182/ D.A. Powers, D.A. Dahlgren, J.F. Muir, W.B. Murfin:  
Exploratory Study of Molten Core Material/Concrete Inter-  
actions;  
July 1975 - March 1977, Sandia Laboratories, SAND77-2042.
- /183/ M. Reimann, W.B. Murfin:  
Calculations for the Decomposition of Concrete Structures  
by a Molten Pool; in /4/, pp. 240-252.
- /184/ J.F. Muir:  
Response of Concrete Exposed to a High Heat Flux on One  
Surface; Sandia Laboratories SAND 77-1467.

- /185/ P.D. Capp, J.M. James, A. Kingsburry, D.L.G. Smith:  
Sacrificial Material/Uranium Dioxide Interactions Experimental  
Studies at AEE Winfrith; in /4/, pp. 325-335.
- /186/ D. Perinic, B. Kammerer, H. Knauß, A. Mack, B. Stuka:  
Betontiegel-Versuche mit Thermitschmelzen;  
KfK 2572, Kernforschungszentrum Karlsruhe, Juli 1979.
- /187/ M. Peehs, G. Hofer, H.J. Friedrich, H.J. Heuvel:  
Experimental Investigations on the Compatibility of a SNR-  
Type Corium with Graphite; in /8/, pp. 2077-2086.
- /188/ J.K. Fink, J.J. Heiberger, L. Lerbowitz:  
Studies of the Rate of Molten Materials in Interactions with  
UO<sub>2</sub> and Graphite; in /9/, pp. 2134-2139.
- /189/ M. Dalle Donne, S. Dorner, A. Roht, H. Werle:  
Further Work on Sodium Borates as Sacrificial Materials for  
a Core-Catcher; in /10/, pp. III-467-474.
- /190/ M.G. Barker, P.G. Gadd:  
A Chemical Study of the Sodium-Concrete Reaction;  
in /10/, pp. III 91-107.
- /191a/ R.P. Colburn, L.D. Mühlestein, J.A. Hassberger, A.J. Mahnke:  
Sodium Concrete Reactions; in /9/, pp. 2093-2102.
- /191b/ A.J. Mahnke, L.D. Mühlestein, R.W. Wierman, R.P. Colburn:  
Breeder Reactor Faulted Cavity Liner Feature Tests;  
in /9/, pp. 2103-2112.

- /192/ R.U. Acton, R.A. Sallach, J.E. Smaardyk, L.A. Kent:  
Sodium Interaction with Concrete and Firebrick;  
in /9/, pp. 2122-2133.
- /193/ A. Suo-Antilla, J.E. Smaardyk:  
Experimental and Analytical Studies of Sodium Interactions  
with Various Concretes; in /10/, pp. III 55-63.
- /194/ J. Dufresne, J. Fermandjian, C. Casselman, J.C. Malet,  
M. Bolvin, Mme Herber:  
Sodium Concrete Interaction; in /10/, pp. III 109-119.
- /195/ D.H. Nguyen, L.D. Muhlestein, A.K. Postma:  
Sodium-Concrete Reaction Model Development; in /10/,  
pp. III 143-152.
- /196/ J.K. Fink, J.J. Heiberger, R. Cumar, R. Blomquist:  
Interaction of Refractories and Reactor Materials with Sodium;  
Trans. Am. Nucl. Soc., Vol. 23, 1976, p. 365.
- /197/ G. Kayser, C. Le Rigoleur:  
PAHR-Engineering Problems and Solutions; in /5/, pp. 345-354.
- /198/ G. Kayser, C. Le Rigoleur, P. Permezel:  
Thermo-Mechanical Loadings of Primary Structures in Accidental  
Conditions and an Approach to Solution by Limit Design;  
Seminaire Post SMIRT "CONFABRE-3" Confinement des Reacteurs  
Rapides, Ispra 1981.

- /199a/ H. Vossebrecker:  
Private Communication, 1981.
- /199b/ K.H. Kerz, H. Laue:  
Mechanical Behaviour of SNR-300 Reactor Vessel Components  
unter PAHR-Conditions; in /5/, pp. 334-335.
- /200/ C. Le Rigoleur, D. Tenchine:  
Sodium Natural Convection Heat Transfers Around the Internal  
Core Catcher in Super Phenix I. Experimental Results and  
Evaluation for Reactor Conditions; in /10/, pp. IV 53-65.
- /201/ N.W. Davies, N. Sheriff:  
An Experimental Investigation of Natural Convection Heat  
Transfer from Downward Facing Surfaces in Sodium for Fast  
Reactor Internal Core Catchers;  
in "Heat Transfer in Nuclear Reactor Safety" Ed. Bankoff and  
Afgan, 1982, Hemisphere Publishing Corporation, pp. 851-865.
- /202/ T. Schulenberg:  
Natural Convection Heat Transfer to Liquid Metals Below  
Downward Facing Horizontal Surfaces; accepted for publica-  
tion in the Int. J. Heat Mass Transfer, 1983.

- /203/ R. Singer, D. Grand, R. Martin:  
Natural Circulation Heat Transfer in Poole-Type LMFBR's;  
in: "Thermal and Hydraulic Aspects of Nuclear Reactor Safety"  
Vol. 2, Liquid Metal Fast Breeder Reactors, Editors O.C. Jones,  
S.G. Bankoff, ASME New York 1977, pp. 239-264.
- /204/ S.L. Addition, E.A. Partiale:  
Natural Circulation in FFTF a Loop Type LMFBR;  
in "Thermal and Hydraulic Aspects of Nuclear Reactor Safety",  
Vol. 2, Liquid Metal Fast Breeder Reactors, Editors O.C. Jones,  
S.G. Bankoff ASME New York 1977, pp. 265-283.
- /205/ R. Webster:  
Convective Flows During Low Power Natural Circulation Experi-  
ments on the PFR; in /10/, pp. II 535-549.
- /206/ W.T. Sha, A. Amorosi, S.S. Borys:  
Three-Dimensional Analysis of LMFBR Decay Heat Removal System;  
in /10/, pp. II 593-60.2.
- /207/ T. Fujii, H. Honda, I. Morioka:  
A Theoretical Study of Natural Convection Heat Transfer from  
Downward Facing Horizontal Surfaces with Uniform Heat Flux;  
Int. J. Heat Mass Transfer, 16, 1973, pp. 611-627.
- /208/ D. Tenchine, M. Amblard:  
Heat Transfer by Natural Convection in Sodium from Downward  
Facing Surfaces; Second Int. Topical Meeting on Nuclear  
Reactor Thermal Hydraulics, Santa Barbara, USA, Jan. 11-14,  
1983.

- /209/ L. Barleon, K. Thomauske, H. Werle:  
Cooling of Debris Beds; Submitted for Publication to  
Nuclear Technolgy, 1983.
- /210/ I. Catton, V.K. Dhir, C.W. Somerton, D. Squarer:  
An Experimental Study of Debris Bed Coolability Under Pool  
Boiling Conditions; EPRI, NP-3094, May 1983.
- /211/ J.D. Gabor, M. Epstein, S.W. Jones, J.C. Cassulo:  
Status Report on Limiting Heat Fluxes in Debris Beds;  
ANL/RAS 80-21, Sept. 1980.
- /212/ R.E. Trenberth, G.F. Stevens:  
An Experimental Study of Boiling Heat Transfer and Dryout  
in Heated Particulate Beds; AEEW-R 1342, July 1980.
- /213/ J.O. Jakobsson, I. Catton, D. Squarer:  
The Effect of Pressure on Dryout Heat Flux in a Volume  
Heated Porous Bed; ASME/JSME Thermal Engineering Joint  
Conference Proceedings, Honolulu, Hawaii, March 20-24, 1983,  
pp. 467-472.

Literature Concerning Appendix I

- /A1/ J. Spino, B. Schulz; Rev. Int. Hautes Temp. Refract. 18 (1981), 257-262.
- /A2/ B. Schulz; in: U. Müller, C. Günther (ed.), Proc. 5th PAHR-Meeting, July 1982, Verlag G. Braun, Karlsruhe, 46-52.
- /A3/ D.R. Boyle et al.; J. Nucl. Mat. 29 (1969), 27.
- /A4/ F. Thümler, H. Kleykamp, P. Hofmann; J. Nucl. Mat. 81 (1979), 215.
- /A5/ L. Leibowitz; Report ANL-CEN-RSD-76-1, 1976.
- /A6/ P. Nikolopoulos, B. Schulz; J. Nucl. Mat. 82 (1979), 172-178.
- /A7/ B. Schulz; 8th Europ. Conf. on Thermophys. Properties, Baden-Baden, Sept. 1982, to be publ. in High Temp., High Press.
- /A8/ S. Nazaré, G. Ondracek, B. Schulz; Nucl. Techn. 32 (1977), 239-244.
- /A9/ W.-D. Sältzer; Dissertation Universität Karlsruhe, 1983.
- /A10/ W.-D. Sältzer, B. Schulz; 8th Europ. Conf. on Thermophys. Properties, Baden-Baden, Sept. 1982, to be publ. in High Temp., High Press.

- /A11/ C.S. Kim, R.A. Blomquist, J. Haley, J. Fisher, M.G. Chasanov, L. Leibowitz, Proc. 7th Symp. on Thermophys. Properties, Gaithersburg, ASME, N.Y., (1977), 338-343.
- /A12/ C. Otter, D. Damien; 8th Europ. Conf. on Thermophys. Properties, Baden-Baden, Sept. 1982, to be published in High Temp., High Press.
- /A13/ H.A. Tasman, D. Pel, J. Richter, H.E. Schmidt; 8th Europ. Conf. on Thermophys. Properties, Baden-Baden, Sept. 1982, to be published in High Temp., High Press.